Impurity-induced quasiparticle transport and universal-limit Wiedemann-Franz violation in *d*-wave superconductors

Adam C. Durst and Patrick A. Lee
Department of Physics, Massachusetts Institute of Technology, Cambridge, Massachusetts 02139
(Received 16 August 1999; revised manuscript received 11 January 2000)

Due to the node structure of the gap in a *d*-wave superconductor, the presence of impurities generates a finite density of quasiparticle excitations at zero temperature. Since these impurity-induced quasiparticles are both generated and scattered by impurities, prior calculations indicate a universal limit ($\Omega \to 0$, $T \to 0$) where the transport coefficients obtain scattering-independent values, depending only on the velocity anisotropy v_f/v_2. We improve upon prior results, including the contributions of vertex corrections and Fermi-liquid corrections in our calculations of universal-limit electrical, thermal, and spin conductivity. We find that while vertex corrections modify electrical conductivity and Fermi-liquid corrections renormalize both electrical and spin conductivity, only thermal conductivity maintains its universal value, independent of impurity scattering or Fermi-liquid interactions. Hence, low-temperature thermal conductivity measurements provide the most direct means of obtaining the velocity anisotropy for high-T_c cuprate superconductors.

I. INTRODUCTION

The characteristic feature of a *d*-wave superconductor is the existence of four nodal points where the order parameter vanishes. Since low-energy excitations are concentrated about these nodes, low-temperature behavior is dominated by the details of the node structure, and, in particular, the ratio of the Fermi velocity to the gap velocity (slope) v_f/v_2. Prior theoretical work has shown that this velocity ratio is prominent in expressions for low-temperature transport coefficients[1–7] as well as the temperature dependence of the superfluid density.[8–10] However, discrepancies between values of v_f/v_2 obtained from measurements of microwave electrical conductivity,[11] thermal conductivity,[12,13] and superfluid density[14], as well as direct measurements of gap structure via angle-resolved photoemission spectroscopy (ARPES)[15] indicate that the existing theoretical predictions must be corrected through a more detailed analysis. To this end, we calculate herein electrical, thermal, and spin conductivity including the contributions of vertex corrections and Fermi-liquid corrections. Associated calculations of the superfluid density will be pursued in a future investigation.

It has been shown[16] that for a superconductor with $d_{x^2-y^2}$ pairing symmetry, the presence of impurities generates a finite density of quasiparticle states down to zero energy (although the ultra-low-energy regime remains the subject of some debate[17,18]). This results in a unique situation where an increase in impurity density increases the density of quasiparticles while reducing the quasiparticle lifetime. As a result of the cancellation of these opposing effects, ''bare bubble'' conductivity calculations (neglecting the corrections we shall consider) indicate a universal limit ($\Omega \to 0, T \to 0$) where the transport coefficients attain constant values, independent of scattering.[1] However, we shall see that these results are modified by two types of corrections: vertex corrections and Fermi-liquid corrections. Vertex corrections account for the fact that forward scattering does not interfere with the progress of a carrier to the same extent as back scattering. Hence, if the scattering potential varies in k space such that the potential for forward scattering differs from that for back scattering, the bare bubble transport coefficients may be modified. Fermi-liquid corrections account for the underlying Fermi-liquid interactions between electrons in the superconductor. Due to such interactions, the presence of a quasiparticle current induces an additional drag current which may renormalize the transport coefficients. The purpose of what follows is to improve upon the bare bubble results by including the effects of both types of corrections.

In Sec. II, we define the parameters of our phenomenological *d*-wave model, introduce the Green's function, and calculate the density of states. In Appendix A, neglecting all corrections, we derive a generalized bare bubble polarization function which can be applied to the calculation of either electrical, thermal, or spin conductivity. By treating the general case, we avoid repeating the same basic calculation three times. In Appendix B, we calculate another generalized polarization function, now including the contributions of vertex corrections. The significance of vertex corrections in the universal limit is determined via a numerical calculation presented in Appendix C. In Appendix D, we derive the renormalization of a generalized current due to the effects of underlying Fermi-liquid interactions. In Secs. III, IV, and V, we make use of the results in the appendices to calculate electrical, thermal, and spin conductivity in the universal limit ($\Omega \to 0, T \to 0$). Each of these sections begins with a derivation of the appropriate current density operator. These calculations reveal an extra gap velocity term in the thermal and spin currents due to the momentum dependence of the *d*-wave gap and therefore indicate a correction to the standard thermal conductivity formula[19,20] derived assuming an *s*-wave gap. Given each current operator, we present the bare bubble result and then note modifications due to vertex corrections and Fermi-liquid corrections. We find that contrary to the scattering-independent result obtained from the bare bubble calculation, the universal limit electrical conductivity attains a vertex correction, which depends explicitly on the nature of the impurity scattering, as well as a Fermi-liquid renormalization, which depends on the strength of Fermi-

liquid interactions. In addition, while the spin conductivity is unaffected by vertex corrections (for small impurity density), it is renormalized due to Fermi-liquid interactions. Only the thermal conductivity has neither a vertex correction nor a Fermi-liquid correction. It therefore retains its simple, universal value. Conclusions are discussed in Sec. VI where we provide physical descriptions of the mathematical corrections calculated herein.

II. D-WAVE MODEL, GREEN'S FUNCTION, AND DENSITY OF STATES

To study the low-temperature transport properties of a *d*-wave superconductor, we employ a phenomenological model[1,8] with the Brillouin zone of a two-dimensional square lattice (of lattice constant a), an electron dispersion (via tight binding parametrization)

$$\epsilon_k = -2t_f(\cos k_x a + \cos k_y a) - \mu, \tag{2.1}$$

and an order parameter of $d_{x^2-y^2}$ symmetry

$$\Delta_k = \frac{\Delta_0}{2}(\cos k_x a - \cos k_y a) \tag{2.2}$$

which crosses through zero at each of four nodal points on the Fermi surface ($k_x = \pm k_y$). The key feature of such a model is that in the vicinity of each of the gap nodes, ϵ_k varies linearly across the Fermi surface and Δ_k varies linearly along the Fermi surface. Defining local momentum variables at each of the nodes with $\hat{\mathbf{k}}_1$ perpendicular to the Fermi surface and $\hat{\mathbf{k}}_2$ parallel to the Fermi surface, we can designate at each node both a Fermi velocity

$$\mathbf{v}_f \equiv \frac{\partial \epsilon_k}{\partial \mathbf{k}} = v_f \hat{\mathbf{k}}_1 \quad v_f = 2\sqrt{2}\, t_f a \tag{2.3}$$

and a gap velocity

$$\mathbf{v}_2 \equiv \frac{\partial \Delta_k}{\partial \mathbf{k}} = v_2 \hat{\mathbf{k}}_2 \quad v_2 = \frac{1}{\sqrt{2}}\Delta_0 a. \tag{2.4}$$

(Note that all velocities in our model are taken to be ''renormalized'' velocities accounting for both band structure and many-body effects within the context of Fermi-liquid theory.) Utilizing these definitions, it becomes clear that the quasiparticle excitation spectrum in the vicinity of each of the gap nodes takes the form of an anisotropic Dirac cone

$$E_k = \sqrt{\epsilon_k^2 + \Delta_k^2} = \sqrt{v_f^2 k_1^2 + v_2^2 k_2^2}, \tag{2.5}$$

where the degree of anisotropy is measured by the ratio of the two velocities. This ratio v_f/v_2 appears prominently in the low-temperature transport coefficients and is a measurable quantity which provides a convenient means of comparing theory to experiment.

The low-temperature physics of such a model is driven by the fact that at the four nodes, there is no gap to quasiparticle excitations. Hence, quasiparticles are generated only in the vicinity of the gap nodes. This is very useful mathematically since it means that a momentum integral over the Brillouin zone can usually be replaced by a sum over nodes and an integral over the small region of k space surrounding each node. Furthermore, due to the form of the excitation spectrum (2.5), it is convenient to scale out the anisotropy of the Dirac cone, and change to polar coordinates in a new scaled momentum $\mathbf{p} = (p, \theta)$. Hence we will frequently make the substitution

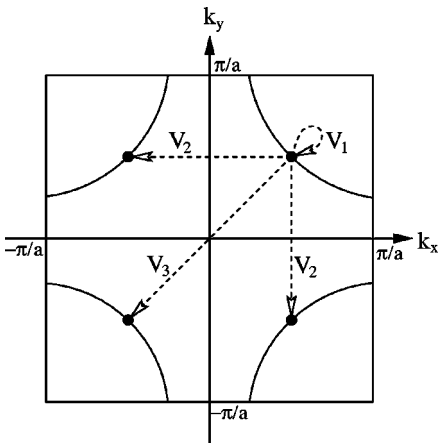

FIG. 1. Impurity scattering within *d*-wave model. V_1, V_2, and V_3 are the potentials for intranode, adjacent-node, and opposite-node scattering.

$$\sum_k \rightarrow \sum_{j=1}^{4} \int \frac{dk_1\, dk_2}{(2\pi)^2} \rightarrow \sum_{j=1}^{4} \int_0^{p_0} \frac{p\, dp}{2\pi v_f v_2} \int_0^{2\pi} \frac{d\theta}{2\pi}, \tag{2.6}$$

where $p_1 = v_f k_1 = p\cos\theta$, $p_2 = v_2 k_2 = p \sin\theta$, $p = \sqrt{p_1^2 + p_2^2} = E_k$, and $p_0 = \sqrt{\pi v_f v_2}/a \sim \mathcal{O}(\Delta_0)$ is a large scaled momentum cutoff defined such that the area of the new integration region is the same as that of the original Brillouin zone. Note that if quasiparticles are only generated at the nodes and the rest of the Brillouin zone makes no contribution, then we should be safe in extending this limit to infinity. However, it is sometimes necessary to retain p_0 through the intermediate stages of a calculation (usually as part of a ratio within a logarithm) maintaining throughout that all other energies are much smaller than this cutoff value.

The fact that quasiparticles are concentrated in the vicinity of the gap nodes is also very useful when considering impurity scattering. Since the initial and final momenta of a scattering event must always be approximately equal to the *k*-space location of one of the four nodes, a general scattering potential, $V_{kk'}$, need only be evaluated in three possible cases: intranode scattering ($\mathbf{k}$ and $\mathbf{k}'$ at the same node), adjacent-node scattering ($\mathbf{k}$ and $\mathbf{k}'$ at adjacent nodes), and opposite-node scattering ($\mathbf{k}$ and $\mathbf{k}'$ at opposite nodes). These are depicted graphically in Fig. 1 and denoted, respectively, as V_1, V_2, and V_3. Hence, an arbitrary potential (varying slowly over the area of a node) is effectively reduced to a set of three parameters. This simplification proves quite helpful.

Since the transport calculations in the sections that follow consist of the evaluation of Feynman diagrams via field-theoretic techniques, it is important to establish the types of Green's functions that will be utilized. For any superconductor, the existence of a condensate of ground state pairs means that the annihilation of an electron must be treated on the same footing as the creation of its mate, an electron with

opposite momentum and spin. Hence we use the Nambu formalism[21] in which the field operators are two-component spinors of the form

$$\Psi_k = \begin{pmatrix} c_{k\uparrow} \\ c^\dagger_{-k\downarrow} \end{pmatrix}, \quad \Psi^\dagger_k = (c^\dagger_{k\uparrow}, c_{-k\downarrow}) \tag{2.7}$$

and the resulting Green's functions are 2×2 matrices in Nambu space. Since we are concerned with finite-temperature calculations, all diagrams will be evaluated using the Matsubara finite temperature formalism.[22] Hence, the bare Matsubara Green's function expressed in Nambu formalism takes the form

$$\tilde{\mathcal{G}}_0(\mathbf{k}, i\omega) = \frac{1}{(i\omega)^2 - E_k^2} \begin{pmatrix} i\omega + \epsilon_k & \Delta_k \\ \Delta_k & i\omega - \epsilon_k \end{pmatrix}, \tag{2.8}$$

where the tilde denotes a Nambu space matrix and $i\omega = i(2n+1)\pi/\beta$ is a fermionic Matsubara frequency. In the presence of impurities, the bare Green's function is dressed via scattering from the impurities and obtains a Matsubara self-energy $\tilde{\Sigma}(i\omega)$. Assuming that all but the scalar component of the self-energy can be neglected or absorbed into ϵ_k or Δ_k, Dyson's equation yields that the dressed Matsubara Green's function is given by

$$\tilde{\mathcal{G}}(\mathbf{k}, i\omega) = \frac{1}{[i\omega - \Sigma(i\omega)]^2 - E_k^2} \times \begin{pmatrix} i\omega - \Sigma(i\omega) + \epsilon_k & \Delta_k \\ \Delta_k & i\omega - \Sigma(i\omega) - \epsilon_k \end{pmatrix}. \tag{2.9}$$

(Note that while this assumption has been explicitly justified in both the Born and unitary scattering limits, the omitted self-energy components can contribute for arbitrary scattering.[23,24] For simplicity, we neglect such contributions in this investigation.) From the Matsubara functions, corresponding retarded functions are obtained by analytically continuing $i\omega \to \omega + i\delta$ such that

$$\tilde{G}_{\rm ret}(\mathbf{k}, \omega) = \tilde{\mathcal{G}}(\mathbf{k}, i\omega \to \omega + i\delta) \tag{2.10}$$

and the impurity scattering rate is defined as

$$\Gamma(\omega) = -\,\mathrm{Im}\,\Sigma_{\rm ret}(\omega) \tag{2.11}$$

where $\Sigma_{\rm ret}(\omega) = \Sigma(i\omega \to \omega + i\delta)$.

With the Green's function in hand, it is a simple and illustrative step to calculate the density of states. In terms of the retarded Green's function, the density of states is given by

$$N(\omega) = -\frac{1}{2\pi} \sum_k \mathrm{Tr}[\,\mathrm{Im}\,\tilde{G}_{\rm ret}(\mathbf{k}, \omega)]. \tag{2.12}$$

Plugging in the Green's function (2.9), replacing the sum by a scaled integral about each node via Eq. (2.6), neglecting the real part of the self-energy, and performing the integration we find that

$$N(\omega) = \frac{2}{\pi^2 v_f v_2} \Gamma(\omega) \left[\ln \frac{p_0}{\Gamma(\omega)} - \ln \sqrt{1 + \frac{\omega^2}{\Gamma(\omega)^2}} \right] + \frac{|\omega|}{\pi v_f v_2} \left[\frac{1}{2} - \frac{1}{\pi} \arctan\left(\frac{\Gamma(\omega)^2 - \omega^2}{2|\omega|\Gamma(\omega)} \right) \right]. \tag{2.13}$$

Note that in the absence of impurities $[\Gamma(\omega) = 0]$,

$$N(\omega)|_{\Gamma(\omega)=0} = \frac{|\omega|}{\pi v_f v_2} \tag{2.14}$$

while in the presence of impurities, there is a finite density of quasiparticle states down to zero energy[16]:

$$N(0) = \frac{2}{\pi^2 v_f v_2} \Gamma_0 \ln \frac{p_0}{\Gamma_0}, \tag{2.15}$$

where $\Gamma_0 \equiv \Gamma(\omega \to 0)$. These *impurity-induced* quasiparticles are responsible for the intriguing low-temperature transport properties that we shall consider in the sections that follow.

III. MICROWAVE ELECTRICAL CONDUCTIVITY

Electrical conductivity can be calculated by means of the Kubo formula[22]

$$\sigma(\Omega, T) = -\frac{\mathrm{Im}\,\Pi_{\rm ret}(\Omega)}{\Omega}, \tag{3.1}$$

where $\Pi_{\rm ret}(\Omega) = \Pi(i\Omega \to \Omega + i\delta)$ and $\Pi(i\Omega)$ is the current-current correlation function (or polarization function) in the Matsubara finite temperature formalism

$$\overleftrightarrow{\Pi}(i\Omega) = -\int_0^\beta d\tau\, e^{i\Omega\tau} \langle T_\tau \mathbf{j}^\dagger(\tau) \mathbf{j}(0) \rangle. \tag{3.2}$$

Thus, our first step is to derive an expression for the electrical current operator. Then by evaluating its correlation function, we obtain the electrical conductivity.

A. Electrical current

For a system of interacting electrons, the Hamiltonian is given by

$$H = \int d\mathbf{x}\, \psi^\dagger_\alpha(\mathbf{x}) \left(\frac{-\nabla^2}{2m^*} \right) \psi_\alpha(\mathbf{x}) + \frac{1}{2} \int d\mathbf{x}\, d\mathbf{y}\, \psi^\dagger_\alpha(\mathbf{x}) \psi^\dagger_\beta(\mathbf{y}) V(\mathbf{x}-\mathbf{y}) \psi_\beta(\mathbf{y}) \psi_\alpha(\mathbf{x}), \tag{3.3}$$

where $\psi_\alpha(\mathbf{x})$ annihilates an electron of spin α at position $\mathbf{x}$ and $V(\mathbf{x}-\mathbf{y})$ is the electron-electron interaction potential. In the presence of a vector potential $\mathbf{A}(\mathbf{x})$, the Hamiltonian must be invariant under a local gauge transformation. While the second term is gauge invariant as written, the first must be modified by making the standard replacement $-i\nabla \to -i\nabla + e\mathbf{A}$. Thus, the Hamiltonian becomes a functional of the vector potential and takes the form

$$H[\mathbf{A}(\mathbf{x})]=\int d\mathbf{x}\,\psi_\alpha^\dagger(\mathbf{x})\left(\frac{(-i\nabla+e\mathbf{A})^2}{2m^*}\right)\psi_\alpha(\mathbf{x})+\frac{1}{2}\int d\mathbf{x}\,d\mathbf{y}\,\psi_\alpha^\dagger(\mathbf{x})\psi_\beta^\dagger(\mathbf{y})V(\mathbf{x}-\mathbf{y})\psi_\beta(\mathbf{y})\psi_\alpha(\mathbf{x}). \tag{3.4}$$

Note that only the kinetic term couples to the vector potential. Taking the functional derivative with respect to $\mathbf{A}(\mathbf{x})$ we obtain an expression for the electrical current:

$$\mathbf{j}^e(\mathbf{x})=-\mathrm{Re}\frac{\delta H}{\delta\mathbf{A}(\mathbf{x})}=\frac{-e}{2im^*}(\psi_\alpha^\dagger\nabla\psi_\alpha-\nabla\psi_\alpha^\dagger\psi_\alpha). \tag{3.5}$$

Then taking the space-time Fourier transform yields

$$\mathbf{j}^e(\mathbf{q},\Omega)=-\frac{e}{m^*}\sum_{k,\omega}\left(\mathbf{k}+\frac{\mathbf{q}}{2}\right)c_{k\alpha}^\dagger c_{k+q\alpha} \tag{3.6}$$

and in the limit that $\mathbf{q}\to 0$ we obtain

$$\mathbf{j}^e(0,\Omega)=-e\sum_{k,\omega}\mathbf{v}_f\Psi_k^\dagger\tilde{\mathbb{I}}\Psi_{k+q}, \tag{3.7}$$

where $\mathbf{v}_f\equiv\partial\epsilon_k/\partial\mathbf{k}=\mathbf{k}/m^*$ and we have expressed the final result in terms of 2×2 Nambu matrix notation. Note that in all cases, momentum indices on field operators denote both momentum and frequency. Although this result is well known, we have derived it here in order to provide a basis for comparison with the thermal current and spin current to be derived later.

B. Bare bubble (electrical)

Given the current, we proceed to calculate the corresponding current-current correlation function. The correlation function for the electrical current can be expressed diagrammatically as a fermionic bubble with fully dressed propagators and a fully dressed vertex in which each vertex contributes a coupling parameter e, a velocity $\mathbf{v}_f$, and a 2×2 Nambu formalism unit matrix $\tilde{\mathbb{I}}$. Assuming that the impurity scattering potential is isotropic in k space, the corrections to the bare vertex vanish. Thus, in this approximation, the conductivity can be obtained from the calculation of a bubble with dressed propagators (i.e., Green's functions with self-energy included) but bare vertices (no interaction between the two propagators). Such a diagram will be referred to as a *bare bubble*.

The calculation of the bare bubble polarization function is of the same basic form for the electrical, thermal, and spin conductivities. Thus, to avoid repeating the same derivation several times, a generalized polarization function $\Pi_{\mathrm{ret}}^{gl\alpha}(\Omega)$ (applicable to all three cases) which depends on a coupling parameter g, a velocity $\mathbf{v}_l$, and a Nambu matrix $\tilde{\tau}_\alpha$ has been calculated in Appendix A. Applying the general result (A13) to the case of interest ($g=e$, $\mathbf{v}_l=\mathbf{v}_f$, $\tilde{\tau}_\alpha=\tilde{\mathbb{I}}$) we find that

$$\sigma(\Omega,T)=\frac{e^2}{\pi^2}\frac{v_f}{v_2}\int\frac{d^2p}{2\pi}\int_{-\infty}^{\infty}d\omega\,\frac{n_F(\omega)-n_F(\omega+\Omega)}{\Omega}\times\mathrm{Tr}[\tilde{G}''_{\mathrm{ret}}(\mathbf{p},\omega)\tilde{G}''_{\mathrm{ret}}(\mathbf{p},\omega+\Omega)], \tag{3.8}$$

where

$$\tilde{G}_{\mathrm{ret}}(\mathbf{p},\omega)=\frac{1}{[\omega-\Sigma_{\mathrm{ret}}(\omega)]^2-p^2}\times\begin{pmatrix}\omega-\Sigma_{\mathrm{ret}}(\omega)+p_1 & p_2\\ p_2 & \omega-\Sigma_{\mathrm{ret}}(\omega)-p_1\end{pmatrix}. \tag{3.9}$$

In the universal limit ($\Omega\to 0, T\to 0$),

$$\frac{n_F(\omega)-n_F(\omega+\Omega)}{\Omega}\to-\frac{\partial n_F}{\partial\omega}\to\delta(\omega). \tag{3.10}$$

Hence, evaluating the rest of the integrand for $\omega\to 0$, noting that $\Sigma_{\mathrm{ret}}(0)=-i\Gamma_0$, and integrating over momentum, we obtain the universal limit bare bubble electrical conductivity

$$\sigma_0=\frac{e^2}{\pi^2}\frac{v_f}{v_2}. \tag{3.11}$$

This is the universal conductivity obtained in Ref. 1. Finite temperature corrections can be obtained via a Sommerfeld expansion [for $T\ll\Gamma(\omega)$] and have been calculated by Hirschfeld *et al.*[3] and Graf *et al.*[5]

C. Vertex corrections (electrical)

The bare bubble conductivity derived above was calculated in the approximation that vertex corrections could be safely neglected. It turns out (as we shall see later) that this approximation is justified if the impurity scattering potential is isotropic in k space ($V_{kk'}=V=\mathrm{const}$). However, for a general scattering potential, corrections to the bare vertex can make a significant contribution and must be included in the calculation. To this end, we shall consider the contribution of the *ladder corrections* to the bare vertex (see Fig. 4 of Appendix B). Once again, since the electrical calculation is of the same form as that for the thermal and spin conductivity, a generalized polarization function including vertex corrections (which can be applied to all three cases) has been calculated in Appendix B. For the electrical conductivity, the polarization function consists of a single bubble (with a dressed vertex) where each vertex contributes a coupling parameter e, a velocity $\mathbf{v}_f$, and a Nambu matrix $\tilde{\mathbb{I}}$. Plugging these parameters into the generalized polarization function (B50) and using the electrical Kubo formula (3.1) we find that

$$\sigma(\Omega,T)=\frac{e^2}{2\pi^2}\frac{v_f}{v_2}\int_{-\infty}^{\infty}d\omega\;\frac{n_F(\omega)-n_F(\omega+\Omega)}{\Omega}\times\mathrm{Re}[J_2^{(0)}(\omega,\Omega)-J_1^{(0)}(\omega,\Omega)], \tag{3.12}$$

where J_1^α and J_2^α are defined in Appendix B. In the universal limit ($\Omega\to 0, T\to 0$), we can make use of Eq. (3.10) to find that

$$\sigma_0=\frac{e^2}{2\pi^2}\frac{v_f}{v_2}\mathrm{Re}\left[\frac{I_2^{(0)}}{1-\gamma_{A2}^{(0)}I_2^{(0)}\{1+(\gamma_{B2}^{(0)}/\gamma_{A2}^{(0)})[\gamma_{B2}^{(0)}I_2^{(1)}/(1-\gamma_{A2}^{(0)}I_2^{(1)})]\}}-\frac{I_1^{(0)}}{1-\gamma_{A1}^{(0)}I_1^{(0)}\{1+(\gamma_{B1}^{(0)}/\gamma_{A1}^{(0)})[\gamma_{B1}^{(0)}I_1^{(1)}/(1-\gamma_{A1}^{(0)}I_1^{(1)})]\}}\right], \tag{3.13}$$

where all functions are evaluated for $\Omega,\omega\to 0$. In these limits, the constituent functions defined in Appendix B take the form

$$F'(0)=\frac{F(i\Gamma_0)}{4\pi v_f v_2}=i\frac{\Gamma_0}{2\pi v_f v_2}\ln\frac{p_0}{\Gamma_0}=i\frac{\pi}{4}N(0), \tag{3.14}$$

$$T_n^a(0)=\left(\frac{\underline{V}}{1+[(\pi/4)N(0)]^2\underline{V}^2}\right)_{n1}\equiv A_n, \tag{3.15}$$

$$T_n^b(0)=i\left(\frac{-(\pi/4)N(0)\underline{V}^2}{1+[(\pi/4)N(0)]^2\underline{V}^2}\right)_{n1}\equiv iB_n, \tag{3.16}$$

$$\gamma_{A1}^{(0)}=\frac{n_i}{4\pi v_f v_2}(A_n^2-B_n^2)[|_{n=1}-|_{n=3}], \tag{3.17a}$$

$$\gamma_{A2}^{(0)}=\frac{n_i}{4\pi v_f v_2}(A_n^2+B_n^2)[|_{n=1}-|_{n=3}], \tag{3.17b}$$

$$\gamma_{B1}^{(0)}=i\frac{n_i}{2\pi v_f v_2}A_nB_n[|_{n=1}-|_{n=3}], \tag{3.17c}$$

$$\gamma_{B2}^{(0)}=0, \tag{3.17d}$$

$$I_1^{(0)}(0,0)=\left.\frac{dF(z)}{dz}\right|_{i\Gamma_0}=2\ln\frac{p_0}{\Gamma_0}-2, \tag{3.18}$$

$$I_2^{(0)}(0,0)=\frac{\mathrm{Im}\,F(i\Gamma_0)}{\Gamma_0}=2\ln\frac{p_0}{\Gamma_0}, \tag{3.19}$$

$$I_1^{(1)}(0,0)=\frac{1}{2}\left(\left.\frac{dF(z)}{dz}\right|_{i\Gamma_0}-\frac{F(i\Gamma_0)}{i\Gamma_0}\right)=-1, \tag{3.20}$$

$$I_2^{(1)}(0,0)=\lim_{\omega\to 0}\frac{\mathrm{Im}[(\omega-i\Gamma_0)F(\omega+i\Gamma_0)]}{2\Gamma_0\omega}=1. \tag{3.21}$$

Thus, including vertex corrections, the universal limit electrical conductivity takes the form

$$\sigma_0=\frac{e^2}{\pi^2}\frac{v_f}{v_2}\beta_{\mathrm{VC}}, \tag{3.22}$$

$$\beta_{\mathrm{VC}}=\frac{1+2[\gamma_{A2}^{(0)}-\gamma_{A1}^{(0)}+\gamma_{B1}^{(0)^2}/(1-\gamma_{A1}^{(0)})]\ln(p_0/\Gamma_0)[\ln(p_0/\Gamma_0)-1]}{[1-2\gamma_{A2}^{(0)}\ln(p_0/\Gamma_0)]\{1-2[\gamma_{A1}^{(0)}-\gamma_{B1}^{(0)^2}/(1-\gamma_{A1}^{(0)})][\ln(p_0/\Gamma_0)-1]\}}, \tag{3.23}$$

where β_{VC} is the scattering-dependent vertex correction to the universal bare bubble result. Note that since the γ's all depend on the difference between the intranode T matrix ($n=1$) and the opposite-node T matrix ($n=3$), $\beta_{\mathrm{VC}}\to 1$ if the two scattering potentials are the same. Hence for an isotropic scattering potential, the bare bubble result (3.11) is recovered. However, in general we presume that the scattering potential will fall off for large **k** and the potential for intranode scattering will be larger than that for opposite-node scattering. If so, the γ's will be nonzero and the universal limit conductivity will deviate from its bare bubble value. This correction to the conductivity due to differences between intranode (forward) scattering and opposite-node (back) scattering is the node-discrete equivalent of the famous $1-\cos\theta$ factor obtained from vertex corrections in the conductivity calculation for a simple metal. As in the metallic case, the phenomenon at work is the fact that forward and back scattering can have different effects on the progress of a charge carrier. As a result, anisotropy in the scattering potential can renormalize the conductivity.

In general, the evaluation of β_{VC} requires a numerical calculation since Γ_0 must be obtained self-consistently as a function of impurity density and scattering potential. Such calculations (presented in Appendix C) indicate that for anisotropic scattering, the electrical vertex correction can be significant even to zeroth order in the impurity density.

For the case of Born scattering, β_{VC} reduces to a more simple and illustrative form. In the Born limit (small V),

$$T_n^a(0)=V_{n1},\quad T_n^b(0)=0, \tag{3.24}$$

$$\gamma_{A1}^{(0)}=\gamma_{A2}^{(0)}=\frac{n_i}{4\pi v_f v_2}(V_1^2-V_3^2),\quad \gamma_{B1}^{(0)}=0, \tag{3.25}$$

and the zero-frequency scattering rate takes the form

$$\Gamma_0 = p_0 \exp\left(-\frac{2\pi v_f v_2}{n_i(V_1^2+2V_2^2+V_3^2)}\right)$$

$$= \frac{\pi}{4} n_i (V_1^2+2V_2^2+V_3^2) N(0), \tag{3.26}$$

where (as defined in Sec. II) V_1, V_2, and V_3 correspond respectively to intranode, adjacent-node, and opposite-node scattering. Noting that $\ln(p_0/\Gamma_0) \sim 1/n_i \gg 1$ and defining

$$\Gamma_1 \equiv 2\gamma_{A1}^{(0)} \Gamma_0 \ln\frac{p_0}{\Gamma_0} = \frac{\pi}{4} n_i (V_1^2 - V_3^2) N(0) \tag{3.27}$$

and a transport scattering rate

$$\Gamma_{tr} \equiv \Gamma_0 - \Gamma_1 = \frac{\pi}{4} n_i (2V_2^2 + 2V_3^2) N(0) \tag{3.28}$$

the vertex correction factor (3.23) reduces to

$$\beta_{\mathrm{VC}} = \left(\frac{\Gamma_0}{\Gamma_{tr}}\right)^2 = \left(\frac{V_1^2+2V_2^2+V_3^2}{2V_2^2+2V_3^2}\right)^2. \tag{3.29}$$

Note that the vertex correction depends on the scattering potential but is independent of the density of impurities. In this simple limit it is clear that if intranode scattering is stronger than opposite-node scattering (as we expect), Γ_0 will exceed Γ_{tr} and the universal limit electrical conductivity will be enhanced beyond the bare bubble result.

D. Fermi-liquid corrections (electrical)

To this point, our calculation of electrical conductivity has neglected the effects of the underlying Fermi-liquid interaction between electrons. In Sec. III A, an explicit expression was derived for the electrical current in the absence of Fermi-liquid interactions. In essence, it has the form

$$\mathbf{j}_0^e = -e \sum_{k\alpha} \mathbf{v}_{fk}\, \delta n_{k\alpha}, \tag{3.30}$$

where $\mathbf{v}_{fk}$ is the Fermi velocity at $\mathbf{k}$ and $\delta n_{k\alpha}$ is the deviation of the electron distribution from equilibrium. The Fermi-liquid renormalization of such a current has been derived in Appendix D. Plugging into the general result (D11) we see that in the presence of Fermi-liquid interactions, the electrical current is given by

$$\mathbf{j}^e = \mathbf{j}_0^e - e\sum_{k'\alpha'} \delta n_{k'\alpha'} \sum_k \mathbf{v}_{fk} f^s_{kk'} \left\{ \frac{\Delta_k^2}{2(\epsilon_k^2+\Delta_k^2)^{3/2}} + \left[\frac{\epsilon_k^2}{E_k^2}\frac{\Gamma_0/\pi}{E_k^2+\Gamma_0^2} - \frac{\Delta_k^2}{\pi E_k^3} \arctan\left(\frac{\Gamma_0}{E_k}\right)\right]\right\}, \tag{3.31}$$

where $f^s_{kk'} = f^{\uparrow\uparrow}_{kk'} + f^{\downarrow\uparrow}_{kk'}$. The first term in brackets is peaked at $\epsilon_k = 0$ and is therefore a Fermi surface term (smeared over the extent of the gap). If we assume a circular Fermi surface, then replacing the k sum by an integral in circular coordinates (k,θ), presuming that $\Delta_k = \Delta(\theta) \ll E_F$, and expanding the Landau function in two-dimensional (2D) harmonics

$$f^s(\theta-\theta') = \frac{1}{\nu(0)} \sum_{l=0}^{\infty} F_l^s \cos[l(\theta-\theta')] \tag{3.32}$$

this first term takes the form

$$\mathbf{j}_1^e = \mathbf{j}_0^e \frac{F_1^s}{2}, \tag{3.33}$$

where F_1^s is the $l=1$ spin-symmetric Landau parameter and $\nu(0)$ is the single spin normal state density of states at the Fermi surface. The second term in brackets is peaked at $E_k = 0$ and is therefore a node term (contributing primarily at the gap nodes). Replacing the k sum by an integral about each of the nodes and noting by symmetry that

$$\sum_{j=1}^{4} \mathbf{v}_f^j f^s_{jj'} = \mathbf{v}_f^{j'} (f^s_{11} - f^s_{31}) \tag{3.34}$$

we find that

$$\mathbf{j}_2^e = -\mathbf{j}_0^e \frac{\Gamma_0 (f^s_{11} - f^s_{31})}{4\pi^2 v_f v_2}, \tag{3.35}$$

where f^s_{11} and f^s_{31} are, respectively, the intranode and opposite-node spin-symmetric Fermi-liquid interaction energies. In the small impurity density limit, the second (node) term can be neglected with respect to the first (Fermi surface) term. Hence, the renormalized electrical current is given by

$$\mathbf{j}^e = \mathbf{j}_0^e \alpha^s_{FL}, \tag{3.36}$$

where (for a circular Fermi surface)

$$\alpha^s_{FL} = 1 + \frac{F_1^s}{2} - \frac{\Gamma_0 (f^s_{11} - f^s_{31})}{4\pi^2 v_f v_2} \approx 1 + \frac{F_1^s}{2} \tag{3.37}$$

and the superscript s denotes that this is the spin-symmetric current renormalization factor. The simple form of this expression is due to our assumption of a circular Fermi surface. For a more general Fermi surface, additional harmonics of the Landau function would have been generated. Thus, in practice, this factor should be treated as a parameter to be determined by experiment. Note that the renormalization applies to both the quasiparticle (normal) current and the supercurrent. However, since the supercurrent does not contribute to the real part of the ac conductivity, we are concerned only with the normal current.

The basic physics of this renormalization is as follows. Upon the application of an electric field, quasiparticles are perturbed to form a normal current. In the presence of the excited quasiparticles, the electron dispersion is modified due to the Fermi-liquid interaction. The modified dispersion yields a modified equilibrium distribution which means that the deviation from equilibrium is also modified and the current is renormalized. Note that the dominant term in the renormalization factor is a Fermi surface term resulting from the modification of the equilibrium condensate distribution in the presence of perturbed quasiparticles.

So far, we have discussed only how Fermi-liquid interactions renormalize the electrical current density operator. Yet our goal is to determine the manner in which such interactions modify the electrical conductivity. In general, such

modifications can be more complicated than merely renormalizing the constituent currents. However, as discussed in Appendix D, current renormalization is the dominant effect in the $T\to 0$ limit with which we are concerned. Therefore, since electrical conductivity is proportional to the current-current correlation function, two powers of our current renormalization factor appear in the conductivity. Hence, including both vertex corrections and Fermi-liquid corrections, the electrical conductivity in the universal limit takes the form

$$\sigma_0 = \frac{e^2}{\pi^2}\frac{v_f}{v_2}\beta_{\rm VC}\alpha_{\rm FL}^{s\,2}. \tag{3.38}$$

E. Superfluid density

As a check on the accuracy of our conductivity calculations, it is useful to make a brief digression and use our results to calculate an experimentally distinct quantity, the superfluid density (without impurities), $\rho^s(T)$. By definition (see Ref. 8),

$$\rho^s(T) \equiv \rho^s(T=0) - \rho^n(T), \tag{3.39}$$

where $\rho^n(T)$ is the normal fluid density. Hence, to obtain the temperature dependence of the superfluid density, it suffices to calculate the normal fluid density. While the conductivity is related to the imaginary part of the polarization function, the normal fluid density is proportional to the real part via

$$\frac{\rho^n(T)}{m} = -\frac{\mathrm{Re}\,\Pi_{\rm ret}(\Omega=0)}{e^2}. \tag{3.40}$$

Obtaining $\Pi_{\rm ret}$ from the generalized result (B49) in Appendix B, setting $\Omega=0$, taking the no impurities limit $[\Gamma(\omega)\to 0]$, and plugging into Eq. (3.40) we find that

$$\frac{\rho^n(T)}{m} = \frac{1}{\pi^2}\frac{v_f}{v_2}\int_{-\infty}^{\infty} d\omega\ \ n_F(\omega)\,\mathrm{Im}[I_1^{(0)}(\omega,0)], \tag{3.41}$$

where

$$\mathrm{Im}[I_1^{(0)}(\omega,0)] = \pi\,\mathrm{sgn}(\omega)[\theta(\omega+p_0)-\theta(\omega-p_0)] + \pi p_0[\delta(\omega+p_0)-\delta(\omega-p_0)]. \tag{3.42}$$

Performing the frequency integration yields that the normal fluid density neglecting Fermi-liquid corrections is given by

$$\frac{\rho^n(T)}{m} = \frac{2\ln 2}{\pi}\frac{v_f}{v_2}k_B T \tag{3.43}$$

which is precisely the result obtained in Ref. 8 through an entirely different procedure. To include Fermi-liquid corrections in the $T\to 0$ limit, we note (via Appendix D) that the primary effect of Fermi-liquid interactions is the renormalization of the current density operator. Thus, since the normal fluid density is proportional to the current-current correlation function, we need only multiply by two factors of the current renormalization (obtained in the previous section) to find that

$$\frac{\rho^n(T)}{m} = \frac{2\ln 2}{\pi}\frac{v_f}{v_2}\alpha_{\rm FL}^{s\,2}k_B T \tag{3.44}$$

which agrees with the results of Refs. 9,10,28. Given this correspondence with prior work, we can be reassured of the accuracy of our calculations.

IV. THERMAL CONDUCTIVITY

Analogous to the case of electrical conductivity, thermal conductivity can be calculated by means of a thermal Kubo formula[22]

$$\frac{\kappa(\Omega,T)}{T} = -\frac{1}{T^2}\frac{\mathrm{Im}\,\Pi^{\kappa}_{\rm ret}(\Omega)}{\Omega}, \tag{4.1}$$

where $\Pi^{\kappa}_{\rm ret}(\Omega)=\Pi^{\kappa}(i\Omega\to\Omega+i\delta)$ and $\Pi^{\kappa}(i\Omega)$ is the finite temperature current-current correlation function (or polarization function). In this case, the appropriate current for the correlation function is the thermal current derived below.

A. Thermal current

To derive an expression for the heat current in an anisotropic superconductor, we can follow the *s*-wave derivation of Ambegaokar and Griffin[19] and generalize to the case of an anisotropic gap. As in Eq. (3.3), the Hamiltonian takes the form

$$H = \int d\mathbf{x}\,\psi_\alpha^\dagger(\mathbf{x})\left(\frac{-\nabla^2}{2m^*}\right)\psi_\alpha(\mathbf{x}) + \frac{1}{2}\int d\mathbf{x}\,d\mathbf{y}\,\psi_\alpha^\dagger(\mathbf{x})\psi_\beta^\dagger(\mathbf{y})V(\mathbf{x}-\mathbf{y})\psi_\beta(\mathbf{y})\psi_\alpha(\mathbf{x}). \tag{4.2}$$

Given the Hamiltonian, it is straightforward to obtain the equations of motion for the field operators

$$i\dot{\psi}_\alpha = [\psi_\alpha, H] = \left(\frac{-\nabla^2}{2m^*} + \int d\mathbf{r}\,V(\mathbf{x}-\mathbf{r})\psi_\gamma^\dagger(\mathbf{r})\psi_\gamma(\mathbf{r})\right)\psi_\alpha \tag{4.3}$$

and to define a Hamiltonian density

$$h(\mathbf{x}) = \frac{1}{2m^*}\nabla\psi_\alpha^\dagger(\mathbf{x})\cdot\nabla\psi_\alpha(\mathbf{x}) + \frac{1}{2}\int d\mathbf{y}\,V(\mathbf{x}-\mathbf{y})\psi_\alpha^\dagger(\mathbf{x})\psi_\beta^\dagger(\mathbf{y})\psi_\beta(\mathbf{y})\psi_\alpha(\mathbf{x}). \tag{4.4}$$

If all energies are measured with respect to the chemical potential, this Hamiltonian density is the heat density. Hence, the operator $\mathbf{j}^Q(\mathbf{x})$ that satisfies the continuity equation

$$\dot{h}(\mathbf{x}) + \nabla\cdot\mathbf{j}^Q(\mathbf{x}) = 0 \tag{4.5}$$

can be interpreted as the heat current. Taking the time derivative of Eq. (4.4) and using the equations of motion (4.3) we find that

$$\dot{h}=\nabla\cdot(\dot{\psi}^{\dagger}_{x\alpha}\nabla\psi_{x\alpha}+\nabla\psi^{\dagger}_{x\alpha}\dot{\psi}_{x\alpha})-\frac{1}{2}\int d\mathbf{y}\,V(\mathbf{y}-\mathbf{x})$$
$$\times[(\dot{\psi}^{\dagger}_{x\alpha}\psi^{\dagger}_{y\beta}\psi_{y\beta}\psi_{x\alpha}+\psi^{\dagger}_{x\alpha}\psi^{\dagger}_{y\beta}\psi_{y\beta}\dot{\psi}_{x\alpha})-(\psi^{\dagger}_{x\alpha}\dot{\psi}^{\dagger}_{y\beta}\psi_{y\beta}\psi_{x\alpha}$$
$$+\psi^{\dagger}_{x\alpha}\psi^{\dagger}_{y\beta}\dot{\psi}_{y\beta}\psi_{x\alpha})], \tag{4.6}$$

where the compact notation $\psi_{x\alpha}\equiv\psi_{\alpha}(\mathbf{x})$ has been used for the sake of brevity. Defining $\mathbf{j}^{Q}=\mathbf{j}^{Q}_{1}+\mathbf{j}^{Q}_{2}$ we can use Eq. (4.5) to write

$$\mathbf{j}^{Q}_{1}(\mathbf{x})=-\frac{1}{2m^{*}}(\dot{\psi}^{\dagger}_{x\alpha}\nabla\psi_{x\alpha}+\nabla\psi^{\dagger}_{x\alpha}\dot{\psi}_{x\alpha}) \tag{4.7}$$

and

$$\nabla\cdot\mathbf{j}^{Q}_{2}(\mathbf{x})=\frac{1}{2}\int d\mathbf{y}\,V(\mathbf{y}-\mathbf{x})$$
$$\times[(\dot{\psi}^{\dagger}_{x\alpha}\psi^{\dagger}_{y\beta}\psi_{y\beta}\psi_{x\alpha}+\psi^{\dagger}_{x\alpha}\psi^{\dagger}_{y\beta}\psi_{y\beta}\dot{\psi}_{x\alpha})$$
$$-(\psi^{\dagger}_{x\alpha}\dot{\psi}^{\dagger}_{y\beta}\psi_{y\beta}\psi_{x\alpha}+\psi^{\dagger}_{x\alpha}\psi^{\dagger}_{y\beta}\dot{\psi}_{y\beta}\psi_{x\alpha})]. \tag{4.8}$$

Taking the space-time Fourier transform of Eq. (4.7) in the limit that $\mathbf{q}\rightarrow 0$ we obtain

$$\mathbf{j}^{Q}_{1}(0,\Omega)=\sum_{k,\omega}\left(\omega+\frac{\Omega}{2}\right)\mathbf{v}_{f}c^{\dagger}_{k\alpha}c_{k+q\alpha}$$
$$=\sum_{k,\omega}\left(\omega+\frac{\Omega}{2}\right)\mathbf{v}_{f}\Psi^{\dagger}_{k}\tilde{\tau}_{3}\Psi_{k+q}, \tag{4.9}$$

where $\mathbf{v}_{f}\equiv\partial\epsilon_{k}/\partial\mathbf{k}=\mathbf{k}/m^{*}$, $c_{k\alpha}$ is the space-time Fourier transform of $\psi_{\alpha}(\mathbf{x})$, and the second line is written in terms of the 2×2 Nambu matrix notation introduced in Sec. II. Please note that in our compact notation, momentum indices on field operators always represent both momentum and frequency [i.e., $\Psi_{k}\equiv\Psi(\mathbf{k},\omega)$ and $\Psi_{k+q}\equiv\Psi(\mathbf{k}+\mathbf{q},\omega+\Omega)$].

Similarly, taking the space-time Fourier transform of Eq. (4.8) generates four terms such that

$$i\mathbf{q}\cdot\mathbf{j}^{Q}_{2}(\mathbf{q},\Omega)=X_{1}+X_{2}-Y_{1}-Y_{2}. \tag{4.10}$$

The first such term, X_{1}, is given by

$$X_{1}=\sum_{k's,\omega's}\omega_{1}V_{k_{5}}c^{\dagger}_{k_{1}\alpha}c^{\dagger}_{k_{2}\beta}c_{k_{3}\beta}c_{k_{4}\alpha}$$
$$\times\delta_{k_{4}-k_{1}-k_{5}-q}\delta_{k_{3}-k_{2}+k_{5}}\delta_{\omega_{1}+\omega_{2}-\omega_{3}-\omega_{4}+\Omega}. \tag{4.11}$$

Taking the mean field approximation, retaining only the terms for which the average values are over $(\mathbf{k}\uparrow,-\mathbf{k}\downarrow)$ pairs, and using the fact that $\langle c^{\dagger}_{k\uparrow}c^{\dagger}_{-k\downarrow}\rangle$ is an even function of ω, this becomes

$$X_{1}=-i\sum_{k,\omega}(\omega-\Omega)\Delta^{\dagger}_{k}c^{\dagger}_{k-q\uparrow}c^{\dagger}_{-k\downarrow}, \tag{4.12}$$

where

$$\Delta_{k}\equiv-\sum_{k',\omega'}V_{k-k'}\langle c^{\dagger}_{k\uparrow}c^{\dagger}_{-k\downarrow}\rangle. \tag{4.13}$$

Repeating this procedure for X_{2}, Y_{1}, and Y_{2} and taking Δ_{k} to be real we find that

$$\mathbf{q}\cdot\mathbf{j}^{Q}_{2}(\mathbf{q},\Omega)=-\sum_{k,\omega}(\Delta_{k+q}-\Delta_{k})$$
$$\times[\omega c^{\dagger}_{k\uparrow}c^{\dagger}_{-(k+q)\downarrow}+(\omega+\Omega)c_{-k\downarrow}c_{k+q\uparrow}]. \tag{4.14}$$

In the limit as $\mathbf{q}\rightarrow 0$

$$\Delta_{k+q}-\Delta_{k}\approx\mathbf{q}\cdot\frac{\partial\Delta_{k}}{\partial\mathbf{k}}\equiv\mathbf{q}\cdot\mathbf{v}_{2}. \tag{4.15}$$

Thus, casting Eq. (4.14) in terms of the Nambu matrix formalism we find that

$$\mathbf{j}^{Q}_{2}(0,\Omega)=-\sum_{k,\omega}\left[\left(\omega+\frac{\Omega}{2}\right)\mathbf{v}_{2}\Psi^{\dagger}_{k}\tilde{\tau}_{1}\Psi_{k+q}\right.$$
$$\left.+\frac{\Omega}{2i}\mathbf{v}_{2}\Psi^{\dagger}_{k}\tilde{\tau}_{2}\Psi_{k+q}\right]. \tag{4.16}$$

In the limit of small Ω, the second term can be neglected compared to the first. Thus, combining Eq. (4.16) with Eq. (4.9) we obtain the following expression for the heat current in an anisotropic superconductor:

$$\mathbf{j}^{Q}(0,\Omega)=\sum_{k,\omega}\left(\omega+\frac{\Omega}{2}\right)[\mathbf{v}_{f}\Psi^{\dagger}_{k}\tilde{\tau}_{3}\Psi_{k+q}-\mathbf{v}_{2}\Psi^{\dagger}_{k}\tilde{\tau}_{1}\Psi_{k+q}]. \tag{4.17}$$

Note that for an *s*-wave superconductor, the gap is independent of $\mathbf{k}$ and $\mathbf{v}_{2}=0$. Thus, the second term in the heat current vanishes and Eq. (4.17) reduces to the result derived by Ambegaokar *et al.*[19,20] However, for a *d*-wave superconductor, the gap is anisotropic and $\mathbf{v}_{2}\neq 0$. Hence, although the gap term may be small, neither term can be formally neglected.

B. Bare bubble (thermal)

Unlike the electrical current, the thermal current has two terms: a ''Fermi'' term proportional to $\mathbf{v}_{f}$ and $\tilde{\tau}_{3}$ and a ''gap'' term proportional to $\mathbf{v}_{2}$ and $\tilde{\tau}_{1}$. Therefore, when we evaluate the current-current correlation function, we expect four bubbles rather than just one: Fermi-Fermi, Fermi-gap, gap-Fermi, and gap-gap. However, since the Fermi velocity $\mathbf{v}_{f}$ and the gap velocity $\mathbf{v}_{2}$ are orthogonal at each of the gap nodes, the two cross terms cancel. Hence, the thermal conductivity has two terms: a Fermi term with velocity $\mathbf{v}_{f}$ and Nambu matrix $\tilde{\tau}_{3}$ on each vertex and a gap term with velocity $\mathbf{v}_{2}$ and Nambu matrix $\tilde{\tau}_{1}$ on each vertex. For both terms the coupling parameter is $(\omega+\Omega/2)$.

Neglecting vertex corrections, each term can be obtained from the bare bubble generalized polarization function derived in Appendix A. Plugging the appropriate parameters into the general result (A13) we find that

$$\frac{\kappa(\Omega,T)}{T}=\frac{1}{\pi^2 v_f v_2}\int\frac{d^2p}{2\pi}\int_{-\infty}^{\infty}d\omega\,\frac{n_F(\omega)-n_F(\omega+\Omega)}{\Omega}\times\left(\frac{\omega+\Omega/2}{T}\right)^2[v_f^2\,\mathrm{Tr}[\tilde{G}''_{\mathrm{ret}}(\mathbf{p},\omega)\tilde{\tau}_3\times\tilde{G}''_{\mathrm{ret}}(\mathbf{p},\omega+\Omega)\tilde{\tau}_3]+v_2^2\,\mathrm{Tr}[\tilde{G}''_{\mathrm{ret}}(\mathbf{p},\omega)\tilde{\tau}_1\times\tilde{G}''_{\mathrm{ret}}(\mathbf{p},\omega+\Omega)\tilde{\tau}_1]]. \tag{4.18}$$

In the universal limit ($\Omega\to 0,\ T\to 0$),

$$\frac{n_F(\omega)-n_F(\omega+\Omega)}{\Omega}\to-\frac{\partial n_F}{\partial\omega} \tag{4.19}$$

which for low T is very sharply peaked at $\omega=0$. Thus, evaluating the rest of the integrand for $\omega\to 0$, noting that $\Sigma_{\mathrm{ret}}(0)=-i\Gamma_0$, performing the frequency integral via

$$\int_{-\infty}^{\infty}\omega^2\left(-\frac{\partial n_F}{\partial\omega}\right)d\omega=\frac{\pi^2}{3}k_B^2T^2 \tag{4.20}$$

and integrating over momentum, we obtain the bare bubble thermal conductivity in the universal limit:

$$\frac{\kappa_0}{T}=\left(\frac{\pi^2}{3}k_B^2\right)\frac{1}{\pi^2}\frac{v_f^2+v_2^2}{v_f v_2}. \tag{4.21}$$

Neglecting the v_2^2 term in the numerator, this result and its finite temperature corrections, were originally calculated by Graf *et al.*[5] The gap term was first obtained by Senthil *et al.*[6] via a physical argument of Wiedemann-Franz correspondence with their expression for spin conductivity. It arises here as a direct result of the additional gap term found in our calculation of the thermal current for a *d*-wave superconductor.

C. Vertex corrections (thermal)

The bare bubble result derived in the previous section can be improved upon by including the contribution of the *ladder corrections* to the bare vertex (see Fig. 4 of Appendix B). A generalized polarization function including such vertex corrections has been derived in Appendix B. By plugging the appropriate parameters into this general formula (B50) both terms of the thermal conductivity (the Fermi term with parameters $\mathbf{v}_f$, $\tilde{\tau}_3$, and $\omega+\Omega/2$ and the gap term with parameters $\mathbf{v}_2$, $\tilde{\tau}_1$, and $\omega+\Omega/2$) can be obtained. Hence we find that

$$\frac{\kappa(\Omega,T)}{T}=\frac{1}{2\pi^2 v_f v_2}\int_{-\infty}^{\infty}d\omega\ \frac{n_F(\omega)-n_F(\omega+\Omega)}{\Omega}\times\left(\frac{\omega+\Omega/2}{T}\right)^2[v_f^2\,\mathrm{Re}[J_2^{(3)}(\omega,\Omega)-J_1^{(3)}(\omega,\Omega)]+v_2^2\,\mathrm{Re}[J_2^{(1)}(\omega,\Omega)-J_1^{(1)}(\omega,\Omega)]], \tag{4.22}$$

where J_1^{α} and J_2^{α} are defined in Appendix B. In the universal limit ($\Omega\to 0,\ T\to 0$), the Fermi function factor is sharply peaked at $\omega=0$. Thus, evaluating the J functions for $\Omega,\omega\to 0$, performing the frequency integral via Eq. (4.20), and noting that

$$J_2^{(3)}(0,0)=-J_1^{(1)}(0,0),\qquad J_1^{(3)}(0,0)=-J_2^{(1)}(0,0) \tag{4.23}$$

we find that the universal limit thermal conductivity takes the form

$$\frac{\kappa_0}{T}=\left(\frac{\pi^2}{3}k_B^2\right)\frac{1}{\pi^2}\frac{v_f^2+v_2^2}{v_f v_2}\beta_{\mathrm{VC}}^T \tag{4.24}$$

$$\beta_{\mathrm{VC}}^T=\frac{1/2}{1-\gamma_{A2}^{(0)}}+\frac{\frac{1}{2}}{1+\gamma_{A1}^{(0)}\left(1+\left(\gamma_{B1}^{(0)}/\gamma_{A1}^{(0)}\right)\left\{\gamma_{B1}^{(0)}[2\ln(p_0/\Gamma_0)-2]/[1-\gamma_{A1}^{(0)}[2\ln(p_0/\Gamma_0)-2]]\right\}\right)}, \tag{4.25}$$

where β_{VC}^T is the thermal vertex correction factor and the γ's are defined in Eq. (3.17). As for the electrical case, the thermal vertex correction must generally be evaluated numerically. The results of such numerical calculations (presented in Appendix C) can be summarized as follows. (1) For all scattering strengths (from Born to unitary) the thermal vertex correction is negligible compared to the electrical vertex correction. (2) In the small impurity density limit, β_{VC}^T-1 vanishes approximately as $[\ln(p_0/\Gamma_0)]^{-1}$. Thus, to zeroth order in the density of impurities, vertex corrections do not contribute. Hence,

$$\beta_{\mathrm{VC}}^T\approx 1 \tag{4.26}$$

and the universal-limit thermal conductivity takes its bare bubble form

$$\frac{\kappa_0}{T}=\left(\frac{\pi^2}{3}k_B^2\right)\frac{1}{\pi^2}\frac{v_f^2+v_2^2}{v_f v_2}. \tag{4.27}$$

This is in stark contrast to the case of electrical conductivity where we found a significant vertex correction even to zeroth order in the impurity density.

D. Fermi-liquid corrections (thermal)

As discussed in Appendix D, there may be additional corrections to the thermal conductivity due to underlying Fermi-liquid interactions between electrons. In the $T\to 0$ limit, the dominant effect of such interactions is to renormalize the current density operator. From (4.17) we see that the thermal current (in the absence of Fermi-liquid interactions) has a rather complicated form including both a Fermi velocity term and a gap velocity term. However, for the purposes of

this analysis, it suffices to neglect the gap term (since it is known to be much smaller) and note that in essence, the bare thermal current has the form

$$\mathbf{j}_0^Q = \sum_{k\alpha} \epsilon_k \mathbf{v}_{fk}\, \delta n_{k\alpha}, \tag{4.28}$$

where $\delta n_{k\alpha}$ is the deviation of the electron distribution from equilibrium. To account for the effects of the Fermi-liquid interactions, a general renormalization factor has been derived in Appendix D. Plugging the appropriate parameters into Eq. (D11) we find that the dressed thermal current is given by

$$\mathbf{j}^Q = \mathbf{j}_0^Q + \sum_{k'\alpha'} \delta n_{k'\alpha'} \sum_k \epsilon_k \mathbf{v}_{fk} f^s_{kk'} \left\{ \frac{\Delta_k^2}{2(\epsilon_k^2+\Delta_k^2)^{3/2}} + \left[\frac{\epsilon_k^2}{E_k^2}\frac{\Gamma_0/\pi}{E_k^2+\Gamma_0^2} - \frac{\Delta_k^2}{\pi E_k^3}\arctan\left(\frac{\Gamma_0}{E_k}\right)\right]\right\}, \tag{4.29}$$

where $f^s_{kk'} = f^{\uparrow\uparrow}_{kk'} + f^{\downarrow\uparrow}_{kk'}$. Since the entire summand is odd in ϵ_k, the correction to the bare current integrates to zero. Hence, at least in the zero temperature limit, the thermal current is not renormalized by Fermi-liquid effects:

$$\mathbf{j}^Q = \mathbf{j}_0^Q. \tag{4.30}$$

Basically, due to the symmetry of the electron dispersion about the Fermi surface, corrections to the thermal current cancel. Since the thermal current is unmodified, there are no Fermi-liquid corrections to the universal limit thermal conductivity. Thus, including both vertex corrections and Fermi-liquid corrections, the thermal conductivity retains the bare bubble form

$$\frac{\kappa_0}{T} = \left(\frac{\pi^2}{3}k_B^2\right)\frac{1}{\pi^2}\frac{v_f^2+v_2^2}{v_f v_2}. \tag{4.31}$$

V. SPIN CONDUCTIVITY

For the spin conductivity case, the Kubo formula takes the form

$$\sigma^s(\Omega,T) = -\frac{\mathrm{Im}\,\Pi^s_{\mathrm{ret}}(\Omega)}{\Omega}, \tag{5.1}$$

where $\Pi^s_{\mathrm{ret}}(\Omega) = \Pi^s(i\Omega \to \Omega + i\delta)$ and $\Pi^s(i\Omega)$ is the finite temperature current-current correlation function (or polarization function). Here the current that enters the correlation function is the spin current derived below.

A. Spin current

To find an expression for the spin current operator in an anisotropic superconductor, we can write down the Hamiltonian and spin density operators and use the spin continuity equation to obtain the current. For spin, the continuity equation is

$$\dot{\rho}^s(\mathbf{x}) = -\nabla\cdot\mathbf{j}^s(\mathbf{x}), \tag{5.2}$$

where ρ^s is the spin density and $\mathbf{j}^s$ is the spin current density. The spin density equation of motion takes the standard form

$$\dot{\rho}^s(\mathbf{x}) = -i[\rho^s(\mathbf{x}), H]. \tag{5.3}$$

Thus, combining the two equations and using a Fourier representation for both the spin density and the spin current we find that

$$\mathbf{q}\cdot\mathbf{j}^s_q = [\rho^s_q, H]. \tag{5.4}$$

The Fourier transform of the spin density operator is given by

$$\rho^s_q = \sum_{k,\omega,\alpha} S_\alpha c^\dagger_{k\alpha} c_{k+q\alpha} = s\sum_{k,\omega}\,(c^\dagger_{k\uparrow}c_{k+q\uparrow} - c^\dagger_{-k\downarrow}c_{-k+q\downarrow}), \tag{5.5}$$

where $S_\alpha = \pm\frac{1}{2}$ and $s \equiv \frac{1}{2}$. In the mean field approximation, the Hamiltonian for a superconductor is expressed as

$$H = \sum_{k,\omega}\,[\epsilon_k(c^\dagger_{k\uparrow}c_{k\uparrow} + c^\dagger_{-k\downarrow}c_{-k\downarrow}) - \Delta_k(c^\dagger_{k\uparrow}c^\dagger_{-k\downarrow} + c_{-k\downarrow}c_{k\uparrow})]. \tag{5.6}$$

Thus, evaluating the commutator of Eqs. (5.5) and (5.6) using fermionic anticommutation relations we obtain

$$\mathbf{q}\cdot\mathbf{j}^s_q = s\sum_{k,\omega}\,[(\epsilon_{k+q}-\epsilon_k)(c^\dagger_{k\uparrow}c_{k+q\uparrow} - c_{-k\downarrow}c^\dagger_{-(k+q)\downarrow}) - (\Delta_{k+q}-\Delta_k)(c^\dagger_{k\uparrow}c^\dagger_{-(k+q)\downarrow} + c_{-k\downarrow}c_{k+q\uparrow})]. \tag{5.7}$$

In the limit as $q \to 0$

$$\epsilon_{k+q} - \epsilon_k \approx \mathbf{q}\cdot\frac{\partial\epsilon_k}{\partial\mathbf{k}} \equiv \mathbf{q}\cdot\mathbf{v}_f, \tag{5.8}$$

$$\Delta_{k+q} - \Delta_k \approx \mathbf{q}\cdot\frac{\partial\Delta_k}{\partial\mathbf{k}} \equiv \mathbf{q}\cdot\mathbf{v}_2. \tag{5.9}$$

Hence, expressing the creation and annihilation operators in terms of 2×2 Nambu matrix notation we find that

$$\mathbf{j}^s(0,\Omega) = s\sum_{k,\omega}\,[\mathbf{v}_f\Psi^\dagger_k\tilde{\tau}_3\Psi_{k+q} - \mathbf{v}_2\Psi^\dagger_k\tilde{\tau}_1\Psi_{k+q}]. \tag{5.10}$$

Note that the spin current takes precisely the same form as the thermal current (4.17) with an appropriate change of coupling parameter.

B. Bare bubble (spin)

As in the thermal conductivity case, the spin current has both a ''Fermi'' term and a ''gap'' term. Hence, evaluating the current-current correlation function and noting (as before) that the cross-terms cancel, we find that the spin conductivity consists of two bubbles: a Fermi term with $\mathbf{v}_f$ and $\tilde{\tau}_3$ on each vertex and a gap term with $\mathbf{v}_2$ and $\tilde{\tau}_1$ on each vertex. These are precisely the bubbles that we evaluated for the thermal case except that here the coupling constant is the spin ($s = 1/2$) rather than the frequency.

Neglecting vertex corrections, each of the two bubbles can be evaluated by plugging the appropriate set of parameters into the bare bubble generalized polarization function (A13) derived in Appendix A. Doing so we find that

$$\sigma^s(\Omega,T)=\frac{s^2}{\pi^2 v_f v_2}\int\frac{d^2p}{2\pi}\int_{-\infty}^{\infty}d\omega\,\frac{n_F(\omega)-n_F(\omega+\Omega)}{\Omega}\times\{v_f^2\,\mathrm{Tr}[\tilde{G}''_{\mathrm{ret}}(\mathbf{p},\omega)\tilde{\tau}_3\tilde{G}''_{\mathrm{ret}}(\mathbf{p},\omega+\Omega)\tilde{\tau}_3]+v_2^2\,\mathrm{Tr}[\tilde{G}''_{\mathrm{ret}}(\mathbf{p},\omega)\tilde{\tau}_1\tilde{G}''_{\mathrm{ret}}(\mathbf{p},\omega+\Omega)\tilde{\tau}_1]\}. \tag{5.11}$$

In the universal limit ($\Omega\to 0, T\to 0$),

$$\frac{n_F(\omega)-n_F(\omega+\Omega)}{\Omega}\to-\frac{\partial n_F}{\partial\omega}\to\delta(\omega). \tag{5.12}$$

Thus, evaluating the rest of the integrand in the $\omega\to 0$ limit, noting that $\Sigma_{\mathrm{ret}}(0)=-i\Gamma_0$, and integrating over momentum, we obtain the universal limit bare bubble spin conductivity:

$$\sigma_0^s=\frac{s^2}{\pi^2}\frac{v_f^2+v_2^2}{v_f v_2}. \tag{5.13}$$

This agrees (aside from a disputed factor of 2) with the result obtained by Senthil *et al.*[6]

C. Vertex corrections (spin)

As in the electrical and thermal cases discussed previously, the bare bubble result derived above can be improved upon by including the contribution of the ladder corrections to the bare vertex. By plugging the appropriate parameters into the generalized polarization function (including vertex corrections) derived in Appendix B, both the Fermi term and the gap term of the spin conductivity can be obtained. Doing so we find that

$$\sigma^s(\Omega,T)=\frac{s^2}{2\pi^2 v_f v_2}\int_{-\infty}^{\infty}d\omega\;\frac{n_F(\omega)-n_F(\omega+\Omega)}{\Omega}\times\{v_f^2\,\mathrm{Re}[J_2^{(3)}(\omega,\Omega)-J_1^{(3)}(\omega,\Omega)]+v_2^2\,\mathrm{Re}[J_2^{(1)}(\omega,\Omega)-J_1^{(1)}(\omega,\Omega)]\}, \tag{5.14}$$

where J_1^α and J_2^α are defined in Appendix B. In the universal limit ($\Omega\to 0, T\to 0$), we can make use of Eq. (5.12) to evaluate the frequency integral and find that

$$\sigma_0^s=\frac{s^2}{\pi^2}\frac{v_f^2+v_2^2}{v_f v_2}\beta^s_{\mathrm{VC}}, \tag{5.15}$$

where the spin vertex correction factor β^s_{VC} is identical to the thermal vertex correction factor β^T_{VC} defined in Eq. (4.25). Thus, mirroring the analysis described in Sec. IV C, we note that for small impurity density, $\beta^s_{\mathrm{VC}}\approx 1$ and the universal limit spin conductivity takes its bare bubble form

$$\sigma_0^s=\frac{s^2}{\pi^2}\frac{v_f^2+v_2^2}{v_f v_2}. \tag{5.16}$$

As in the thermal case and in contrast to the electrical case, vertex corrections do not contribute (to zeroth order in the impurity density).

D. Fermi-liquid corrections (spin)

An additional correction to the spin conductivity is needed to account for the effects of underlying Fermi-liquid interactions between electrons. In the $T\to 0$ limit, the dominant effect of Fermi-liquid interactions is the renormalization of the current density operator (see Appendix D). Neglecting the gap term in Eq. (5.10) (since it is small and rather difficult to deal with), the spin current has the basic form

$$\mathbf{j}_0^s=\sum_{k\alpha}S_\alpha\mathbf{v}_{fk}\,\delta n_{k\alpha}, \tag{5.17}$$

where $S_\alpha=\pm 1/2$. The Fermi-liquid renormalization of this current can then be obtained by plugging the appropriate parameters into the general result (D11) derived in Appendix D. Noting that the math is completely analogous to that of the electrical calculation in Sec. III D, we can easily adapt the electrical result to the present case. Replacing $-e$ with s $(=1/2)$ and changing spin-symmetric designations to spin-antisymmetric ones, we find that the Fermi liquid renormalization of the spin current takes the form

$$\mathbf{j}^s=\mathbf{j}_0^s\alpha^a_{\mathrm{FL}}, \tag{5.18}$$

where α^a_{FL} is the spin-antisymmetric current renormalization factor which, for a general Fermi surface, is some complicated function of the spin-antisymmetric Landau parameters F_l^a. For the simplified case of a circular Fermi surface

$$\alpha^a_{\mathrm{FL}}\approx 1+\frac{F_1^a}{2}. \tag{5.19}$$

As in the electrical case, the current renormalization is dominated by a Fermi surface term resulting from the interaction-induced modification of the equilibrium distribution of the condensate. At first glance, this result is a bit surprising since the Zeeman field which generates the (normal) spin current cannot induce a supercurrent. However, it must be understood that the renormalization of the normal current has nothing to do with the presence of a supercurrent. Rather, due to the existence of the normal current, the *equilibrium* distribution of the condensate is modified (via Fermi-liquid effects). It is this modification of the equilibrium condensate, not the presence of an excited condensate (supercurrent), that gives rise to the renormalization of the spin current.

Since the spin conductivity is proportional to the current-current correlation function, it obtains two factors of the spin current renormalization. Thus, including both vertex corrections and Fermi-liquid corrections, the universal limit spin conductivity takes the form

$$\sigma_0^s=\frac{s^2}{\pi^2}\frac{v_f^2+v_2^2}{v_f v_2}{\alpha^a_{\mathrm{FL}}}^2. \tag{5.20}$$

VI. CONCLUSIONS

In the presence of impurities, the gap symmetry of a *d*-wave superconductor yields the generation of impurity-induced quasiparticles at the gap nodes. The transport properties of the resulting system are quite unique since such quasiparticles are both generated and scattered by impurities. In the $\Omega \to 0, T \to 0$ limit, bare bubble calculations indicate that transport coefficients are ''universal,'' independent of the impurity density or scattering rate. However, once the contributions of vertex corrections and Fermi liquid corrections are included, we find that (putting in the $\hbar$'s) the electrical, thermal, and spin conductivities in this universal limit take the form

$$\sigma_0 = \frac{e^2}{\hbar \pi^2} \frac{v_f}{v_2} \beta_{\rm VC} {\alpha^s_{\rm FL}}^2, \tag{6.1a}$$

$$\frac{\kappa_0}{T} = \frac{[(\pi^2/3)k_B^2]}{\hbar \pi^2} \left(\frac{v_f}{v_2} + \frac{v_2}{v_f} \right), \tag{6.1b}$$

$$\sigma_0^s = \frac{s^2}{\hbar \pi^2} \left(\frac{v_f}{v_2} + \frac{v_2}{v_f} \right) {\alpha^a_{\rm FL}}^2, \tag{6.1c}$$

where $\beta_{\rm VC}$ is a scattering-dependent vertex correction (3.23) and $\alpha^s_{\rm FL}$ and $\alpha^a_{\rm FL}$ are spin-symmetric and spin-antisymmetric Fermi-liquid factors (3.36),(5.18). Note that these are the 2D conductivities of a single CuO_2 plane. To obtain 3D conductivities, they must be multiplied by the number of CuO_2 planes per unit length stacked along the *c* axis.

The ''law'' of Wiedemann and Franz suggests that the transport coefficients should be related such that

$$\frac{\kappa}{\sigma T} = \frac{\pi^2}{3} \frac{k_B^2}{e^2}, \quad \frac{\kappa}{\sigma^s T} = \frac{\pi^2}{3} \frac{k_B^2}{s^2}, \quad \frac{\sigma^s}{\sigma} = \frac{s^2}{e^2}. \tag{6.2}$$

However, examination of the expressions above yields three sources of Wiedemann-Franz violation: current operator definition corrections, vertex corrections, and Fermi-liquid corrections. First of all, since the electrical current has only a Fermi term while the thermal and spin currents include both a Fermi term and a gap term, σ_0 is proportional to the ratio v_f/v_2 while κ_0 and σ_0^s involve an extra v_2/v_f term. These extra terms arise when the thermal and spin current operators are corrected to account for the anisotropy of the order parameter. However, since $v_f/v_2 \sim 14$ for YBCO,[13] this type of violation is of more qualitative than quantitative importance. Secondly, unless impurity scattering is completely isotropic in *k* space, the electrical conductivity contains a scattering-dependent vertex correction $\beta_{\rm VC}$, which cannot be neglected even to zeroth order in impurity density. However, analogous corrections to the thermal and spin conductivities vanish in the small impurity density limit. Thus we expect a scattering-dependent enhancement of σ_0 that is absent in κ_0 and σ_0^s. Finally, due to underlying Fermi-liquid interactions, the electrical and spin conductivities gain spin-symmetric and spin-antisymmetric correction factors, respectively. Corresponding corrections to the thermal current cancel due to particle-hole symmetry. Hence, while Fermi-liquid interactions modify σ_0 and σ_0^s, the value of κ_0 is unaffected.

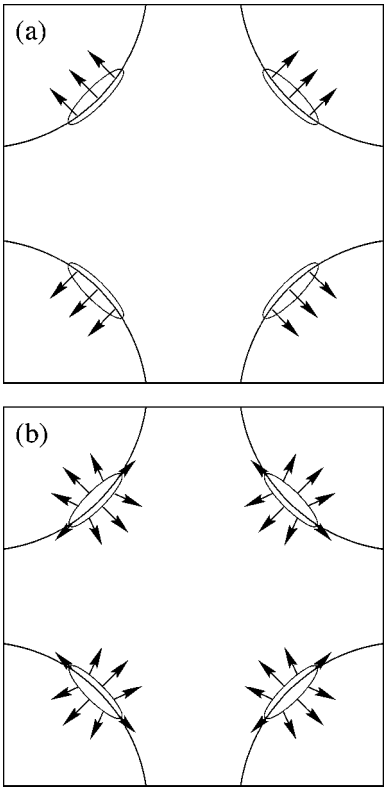

FIG. 2. Schematic depictions of the (a) electrical current and (b) thermal/spin current in the vicinity of the four gap nodes. Electrical current is proportional to the Fermi velocity $\mathbf{v}_f = \partial \epsilon_k / \partial \mathbf{k}$, whereas thermal/spin current is proportional to the group velocity $\mathbf{v}_G = \partial E_k / \partial \mathbf{k}$. The ellipses drawn at each node denote (at a very exaggerated scale) the regions of *k* space within which impurity-induced quasiparticles are generated in the universal limit. [Note that in the small impurity density regime with which we are concerned ($\Gamma_0 \ll \Delta_0$), these nodal regions are pointlike on the scale of the Brillouin zone.]

The physical origin of the first two corrections lies with the velocity dependence of the current operators. Although somewhat obscured in the Nambu formalism, when our current operators (3.7),(4.17),(5.10) are rewritten in the quasiparticle basis, it is clear that the electrical current is proportional to the Fermi velocity $\mathbf{v}_f = \partial \epsilon_k / \partial \mathbf{k}$, while the thermal and spin currents are proportional to the group velocity $\mathbf{v}_G = \partial E_k / \partial \mathbf{k}$. This difference arises because quasiparticles carry definite energy and spin but do not carry definite charge. Since energy and spin are well defined in the quasiparticle basis, thermal and spin currents are proportional to the group velocity, the derivative of the quasiparticle dispersion. By contrast, the electron and hole parts of each quasiparticle have opposite charge and opposite velocity. Therefore each part carries the same electrical current, proportional to the normal state Fermi velocity. This point was emphasized in Ref. 8. For a *d*-wave superconductor where both ϵ_k and Δ_k are momentum dependent, the group velocity will have both a $\mathbf{v}_f$ component and a $\mathbf{v}_2$ component while the Fermi velocity can only have a $\mathbf{v}_f$ component (see Fig. 2). This is the source of the extra gap terms in the thermal and spin conductivities. (Similar conclusions were drawn by Moreno and Coleman.[25])

The role of vertex corrections can be understood by con-

sidering the graphical depictions of the Fermi velocity and group velocity presented in Fig. 2. Throughout the area of a node, the magnitude and direction of the Fermi velocity is approximately constant. Thus, the electrical current can relax much more effectively via scattering from node to node than it can via scattering within a single node. It is therefore necessary to distinguish, mathematically, between the effects of intranode scattering and internode scattering. This is accomplished through the inclusion of vertex corrections. In contrast, the group velocity varies significantly over the area of a node. Therefore, the thermal and spin currents can relax through either intranode scattering or scattering between nodes. As a result, the different types of scattering play nearly the same role and need not be distinguished. Hence, vertex corrections do not contribute to the thermal and spin conductivity.

Fermi-liquid corrections result from the redistribution of equilibrium electrons in response to the presence of interactions between excited electrons. In essence, this redistribution gives rise to a drag current that can renormalize the quasiparticle current and therefore the conductivity. The character of the renormalization depends on the nature of the coupling parameter for a particular current. Since the spin current gets opposite contributions from the two species of spin, the spin conductivity gets a spin-antisymmetric renormalization. However, charge is spin independent so the electrical conductivity gets a spin-symmetric renormalization. Furthermore, since energy changes sign across the Fermi surface, particle-hole symmetry dictates that the effects of Fermi-liquid interactions on the thermal current must cancel. Thus, thermal conductivity is not renormalized.

The velocity ratio v_f/v_2 is a fundamental material parameter which measures the anisotropy of the quasiparticle excitation spectrum. Therefore, an important objective in measuring quantities such as the normal fluid density and the universal limit transport coefficients, which all depend on v_f/v_2, is to obtain the value of this ratio. However, due to vertex corrections and Fermi-liquid corrections, the electrical conductivity, spin conductivity, and normal fluid density depend on parameters (such as interaction energy and/or scattering potential) with values that are not well known. Only the thermal conductivity involves neither vertex corrections nor Fermi-liquid corrections. Thus, κ_0 is the only truly ''universal'' coefficient and is the quantity from which the value of v_f/v_2 can be most directly obtained. On the other hand, the linear T coefficient of the superfluid density (3.44) is proportional to $\alpha_{\mathrm{FL}}^{s\,2} v_f/v_2$. Hence, these two measurements can be combined to determine the Fermi liquid factor α_{FL}^{s}.

In fact, while this paper was in preparation, Chiao *et al.*[26] applied these conclusions to the results of a series of recent experiments performed on optimally doped $Bi_2Sr_2CaCu_2O_8$ (BSCCO). By analyzing the residual linear term in their very low temperature thermal conductivity measurements in terms of Eq. (6.1b), they obtained a value for the velocity ratio, $v_f/v_2=19$. This is roughly the same value obtained from the ARPES measurements of Mesot *et al.*[15] Going further, by combining this result with the linear T coefficient of the superfluid density measured by Waldram and co-workers[27] and making use of Eq. (3.44), they extracted a value for the Fermi-liquid correction $\alpha_{\mathrm{FL}}^{s\,2}=0.43$. These results provide an experimental verification of our analysis.

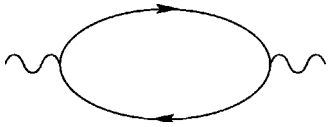

FIG. 3. Bare polarization bubble.

ACKNOWLEDGMENTS

The authors gratefully acknowledge discussions with A. J. Berlinsky, C. Kallin, D. Bonn, and L. Taillefer and helpful comments from M. R. Norman and J. A. Sauls. A.C.D. thanks A. Abanov and M. Oktel for valuable help with calculations. This material is based upon work supported under a National Science Foundation Graduate Fellowship as well as NSF Grant No. DMR-9813764.

APPENDIX A: BARE BUBBLE CALCULATION

In the absence of vertex corrections, our calculations of electrical, thermal, and spin conductivity all require the evaluation of *bare bubble* diagrams depicting various types of polarization functions. The details of these different calculations are all quite similar. They differ only in the coupling parameter, velocity, and Pauli matrix contributed by each bare vertex. Rather than repeating the same basic calculation several times, it is convenient to calculate a generalized polarization function here which can be referred to for each of the specific cases of interest. This generalized function $\overleftrightarrow{\Pi}^{gl\alpha}$, will depend on a coupling parameter g, a velocity $\mathbf{v}_l$, and a Nambu space Pauli matrix $\tilde{\tau}_\alpha$, where

$$g=\{e,s(=1/2),\omega+\Omega/2\},$$

$$\mathbf{v}_l=\{\mathbf{v}_f,\mathbf{v}_2\},$$

$$\tilde{\tau}_\alpha=\{\tilde{\tau}_0(=\tilde{\mathbb{1}}),\tilde{\tau}_1,\tilde{\tau}_2,\tilde{\tau}_3\}.$$

Evaluating the diagram in Fig. 3 we find that

$$\overleftrightarrow{\Pi}^{gl\alpha}(i\Omega)=\frac{1}{\beta}\sum_{k,i\omega} g^2\mathbf{v}_l\mathbf{v}_l\,\mathrm{Tr}[\tilde{\mathcal{G}}(\mathbf{k},i\omega)\tilde{\tau}_\alpha\tilde{\mathcal{G}}(\mathbf{k},i\omega+i\Omega)\tilde{\tau}_\alpha], \tag{A1}$$

where $\tilde{\mathcal{G}}(\mathbf{k},i\omega)$ is the 2×2 Nambu matrix form of the Matsubara Green's function. For a *d*-wave superconductor at temperatures much less than the gap maximum, quasiparticles are generated primarily at the four gap nodes.[1,8] Thus, linearizing the quasiparticle spectrum about the nodes and defining a coordinate system (k_1,k_2) at each node with $\hat{\mathbf{k}}_1$ ($\hat{\mathbf{k}}_2$) perpendicular (parallel) to the Fermi surface, we can replace our momentum sum by an integral over the k space area surrounding each node. If we further define a scaled momentum (p_1,p_2) we can let

$$\sum_k \rightarrow \sum_{j=1}^{4}\int\frac{d^2k}{(2\pi)^2}\rightarrow\sum_{j=1}^{4}\int\frac{d^2p}{(2\pi)^2 v_f v_2}, \tag{A2}$$

where $p_1\equiv v_f k_1=\varepsilon_{\mathbf{k}}$ and $p_2\equiv v_2 k_2=\Delta_{\mathbf{k}}$. Since $\mathbf{v}_f=v_f\hat{\mathbf{k}}_1$ and $\mathbf{v}_2=v_2\hat{\mathbf{k}}_2$ at each of the four nodes, the sum over nodes yields

$$\sum_{j=1}^{4} \mathbf{v}_l^{(j)} \mathbf{v}_l^{(j)} = 2v_l^2 \overleftrightarrow{\mathbb{1}}. \tag{A3}$$

This, in turn, allows the definition of a scalar polarization function via

$$\overleftrightarrow{\Pi}^{gl\alpha}(i\Omega) \equiv \Pi^{gl\alpha}(i\Omega) \overleftrightarrow{\mathbb{1}}. \tag{A4}$$

Defining a spectral representation for $\tilde{\mathcal{G}}$, we can write

$$\tilde{\mathcal{G}}(\mathbf{p}, i\omega) = \int_{-\infty}^{\infty} \frac{\tilde{A}(\mathbf{p}, \omega_1)}{i\omega - \omega_1} d\omega_1, \tag{A5}$$

where

$$\tilde{A}(\mathbf{p}, \omega) = -\frac{1}{\pi} \tilde{G}''_{\mathrm{ret}}(\mathbf{p}, \omega) \tag{A6}$$

and $\tilde{G}''_{\mathrm{ret}}$ is the imaginary part of the retarded Green's function. Plugging back into Eq. (A1) we obtain

$$\Pi^{gl\alpha}(i\Omega) = \frac{2v_l^2}{v_f v_2} \int \frac{d^2p}{(2\pi)^2} \int d\omega_1 \int d\omega_2 \times \mathrm{Tr}[\tilde{A}(\mathbf{p}, \omega_1) \tilde{\tau}_\alpha \tilde{A}(\mathbf{p}, \omega_2) \tilde{\tau}_\alpha] S, \tag{A7}$$

where

$$S = \frac{1}{\beta} \sum_{i\omega} g^2 \frac{1}{i\omega - \omega_1} \frac{1}{i\omega + i\Omega - \omega_2}. \tag{A8}$$

Evaluating the Matsubara sum in the standard way[22] we pick up a contribution from each of the poles of the summand. Since the intermediate results differ depending on the frequency dependence of the coupling parameter, it is best to handle the frequency-independent coupling and frequency-dependent coupling cases separately.

For $g = \{e, s\}$ (frequency-independent coupling), the sum is straightforward. Adding the contribution of the two poles and then continuing $i\Omega \to \Omega + i\delta$ we obtain the retarded function

$$S_{\mathrm{ret}} = S(i\Omega \to \Omega + i\delta) = g^2 \frac{n_F(\omega_1) - n_F(\omega_2)}{\omega_1 - \omega_2 + \Omega + i\delta}, \tag{A9}$$

where

$$n_F(\omega) = \frac{1}{e^{\beta\omega} + 1} \tag{A10}$$

is the Fermi function.

For $g = \omega + \Omega/2$ (frequency-dependent coupling), we proceed in the same way but there are a few technicalities that must be clarified. First of all, it should be understood that within the Matsubara sum we really mean $g \to i\omega + i\Omega/2$. Only after the sum has been evaluated and all frequencies have been continued to the real axis should the stated form of the coupling parameter be taken literally. Secondly, note that with this frequency-dependent g, the summand has two extra powers of frequency. As a result, the sum appears to be divergent. However, as discussed by Ambegaokar and Griffin,[19] this apparent divergence results from an improper treatment of time-derivatives within the time-ordered correlation function and should be ignored. Doing so, we proceed just as before. Adding the contribution of the two summand poles and continuing the external frequency to the real axis we find that

$$S_{\mathrm{ret}} = \frac{(\omega_1 + \Omega/2)^2 n_F(\omega_1) - (\omega_2 - \Omega/2)^2 n_F(\omega_2)}{\omega_1 - \omega_2 + \Omega + i\delta}. \tag{A11}$$

Plugging Eqs. (A9) and (A11) back into Eq. (A7), writing the spectral function in terms of the retarded Green's function via Eq. (A6), and using the identity

$$\frac{1}{x + i\delta} = \mathrm{P}\frac{1}{x} - i\pi\delta(x) \tag{A12}$$

to take the imaginary part, we find that

$$\mathrm{Im}\,\Pi^{gl\alpha}_{\mathrm{ret}}(\Omega) = \frac{1}{\pi^2} \frac{v_l^2}{v_f v_2} \int \frac{d^2p}{2\pi} \int_{-\infty}^{\infty} d\omega \times g^2 [n_F(\omega + \Omega) - n_F(\omega)] \times \mathrm{Tr}[\tilde{G}''_{\mathrm{ret}}(\mathbf{p}, \omega) \tilde{\tau}_\alpha \tilde{G}''_{\mathrm{ret}}(\mathbf{p}, \omega + \Omega) \tilde{\tau}_\alpha] \tag{A13}$$

for all three coupling parameters $g = \{e, s, \omega + \Omega/2\}$. Neglecting vertex corrections, this is the imaginary part of the generalized retarded polarization function. The real part can be obtained via Kramers-Kronig analysis. By specifying different input parameters, Eq. (A13) can be used to obtain the electrical, thermal, and spin conductivity.

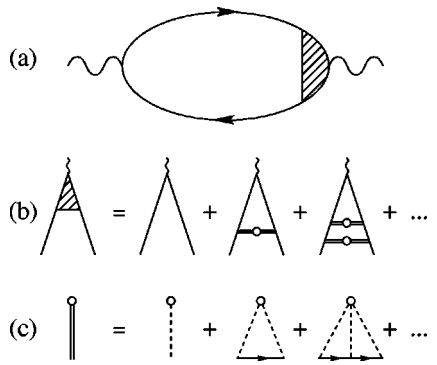

FIG. 4. (a) Polarization bubble with dressed vertex. (b) Ladder series. (c) *T*-matrix series.

APPENDIX B: VERTEX CORRECTIONS

Unless the scattering potential is completely isotropic, the bare bubble results of Appendix A can be improved upon by including the contributions of vertex corrections. In this section the *ladder corrections* depicted in Fig. 4 will be included. Once again, our object is to obtain an expression for a generalized polarization function $\overleftrightarrow{\Pi}^{gl\alpha}$ in which each of the vertices contribute a coupling parameter g, a velocity $\mathbf{v}_l$, and a Nambu space Pauli matrix $\tilde{\tau}_\alpha$. Evaluating the diagram in Fig. 4(a) and noting that $\mathbf{v}_l \equiv v_l \hat{\mathbf{k}}_l$ we find that the generalized polarization function takes the form

$$\overleftrightarrow{\Pi}^{gl\alpha}(i\Omega)=\frac{1}{\beta}\sum_{i\omega}\sum_{k} g^2 v_l^2 \hat{\mathbf{k}}_l \times \mathrm{Tr}[\tilde{\mathcal{G}}(\mathbf{k},i\omega)\tilde{\tau}_\alpha\tilde{\mathcal{G}}(\mathbf{k},i\omega+i\Omega)\tilde{\tau}_\alpha\tilde{\mathbf{\Gamma}}^{l\alpha}(\mathbf{k},i\omega,i\Omega)] \tag{B1}$$

which is equivalent to the bare bubble result (A1) with the unit vector $\hat{\mathbf{k}}_l$ from the second bare vertex replaced by a more general vertex function $\tilde{\mathbf{\Gamma}}^{l\alpha}$. Evaluating the diagram series in Fig. 4(b) we obtain an equation which can be solved for the vertex function

$$\tilde{\tau}_\alpha\tilde{\mathbf{\Gamma}}^{l\alpha}(\mathbf{k})=\hat{\mathbf{k}}_l\tilde{\tau}_\alpha+n_i\sum_{k''}\tilde{T}_{kk''}(i\omega+i\Omega)\tilde{\mathcal{G}}(\mathbf{k}'',i\omega+i\Omega) \times\tilde{\tau}_\alpha\tilde{\mathbf{\Gamma}}^{l\alpha}(\mathbf{k}'')\tilde{\mathcal{G}}(\mathbf{k}'',i\omega)\tilde{T}_{k''k}(i\omega), \tag{B2}$$

where n_i is the impurity density and $\tilde{T}_{kk'}(i\omega)$ is the impurity scattering T matrix defined by the diagram series in Fig. 4(c). Multiplying from the left by $\tilde{\tau}_\alpha$ we can define

$$\tilde{\Gamma}^{l\alpha}(\mathbf{k},i\omega,i\Omega)=\hat{\mathbf{k}}_l[\tilde{\mathbb{1}}+\tilde{\Lambda}^\alpha(i\omega,i\Omega)], \tag{B3}$$

where

$$\hat{\mathbf{k}}_l\tilde{\Lambda}^\alpha=n_i\sum_{k''}\tilde{\tau}_\alpha\tilde{T}_{kk''}(i\omega+i\Omega)\tilde{\mathcal{G}}(\mathbf{k}'',i\omega+i\Omega)\tilde{\tau}_\alpha \times\tilde{\mathbf{\Gamma}}^{l\alpha}(\mathbf{k}'')\tilde{\mathcal{G}}(\mathbf{k}'',i\omega)\tilde{T}_{k''k}(i\omega). \tag{B4}$$

Acting on both sides of Eq. (B3), using Eq. (B4) to replace the left hand side by $\hat{\mathbf{k}}_l'\tilde{\Lambda}^\alpha$, and noting that by the symmetry of the scattering potential

$$\sum_k \hat{\mathbf{k}}_l\rightarrow\hat{\mathbf{k}}_l'\sum_k(\hat{\mathbf{k}}'\cdot\hat{\mathbf{k}}) \tag{B5}$$

we find that

$$\tilde{\Lambda}^\alpha=n_i\sum_k(\hat{\mathbf{k}}'\cdot\hat{\mathbf{k}})\tilde{\tau}_\alpha\tilde{T}_{k'k}(i\omega+i\Omega)\tilde{\mathcal{G}}(\mathbf{k},i\omega+i\Omega)\tilde{\tau}_\alpha \times[\tilde{\mathbb{1}}+\tilde{\Lambda}^\alpha]\tilde{\mathcal{G}}(\mathbf{k},i\omega)\tilde{T}_{kk'}(i\omega), \tag{B6}$$

where $\mathbf{k}'$ is the final momentum of a scattering event.

An expression for the T matrix in terms of the scattering potential $V_{kk'}$ and the Matsubara self-energy $\Sigma(i\omega)$ (itself a function of the scattering potential) can be obtained by evaluating the diagram series in Fig. 4(c):

$$\tilde{T}_{kk'}(i\omega)=\tilde{\tau}_3V_{kk'}+\sum_{k_1}\tilde{\tau}_3\tilde{\mathcal{G}}(\mathbf{k_1},i\omega)\tilde{\tau}_3V_{kk_1}V_{k_1k'}+\cdots. \tag{B7}$$

As discussed in Appendix A, at temperatures low compared to the gap maximum, quasiparticles are only generated in the small regions of k-space surrounding each of the four gap nodes. Hence we can let

$$\sum_k\rightarrow\sum_{j=1}^{4}\int\frac{d^2p}{(2\pi)^2v_fv_2} \tag{B8}$$

and note that the initial and final momenta of a scattering event must always be approximately equal to the k-space location of one of the four nodes. Thus if j and j' are node indices (1 to 4), the scattering potential takes the form

$$V_{kk'}\rightarrow V_{jj'}\rightarrow(\underline{V})_{jj'}, \tag{B9}$$

where $\underline{V}$ is a 4×4 matrix in node space. Due to the symmetry of the nodes, $\underline{V}$ consists of only three independent parameters: V_1 for intranode scattering, V_2 for adjacent-node scattering, and V_3 for opposite-node scattering (see Fig. 1 in Sec. II):

$$\underline{V}=\begin{pmatrix} V_1 & V_2 & V_3 & V_2\\ V_2 & V_1 & V_2 & V_3\\ V_3 & V_2 & V_1 & V_2\\ V_2 & V_3 & V_2 & V_1\end{pmatrix} \tag{B10}$$

Hence Eq. (B7) becomes

$$\tilde{T}_{jj'}(i\omega)=\tilde{\tau}_3(\underline{V})_{jj'}+\tilde{\tau}_3\left(\int\frac{d^2p}{(2\pi)^2v_fv_2}\tilde{\mathcal{G}}(\mathbf{p},i\omega)\right)\tilde{\tau}_3(\underline{V}^2)_{jj'} +\cdots. \tag{B11}$$

Performing the node integration we see that the integral of the Green's function about a node is a scalar in Nambu space (proportional to $\tilde{\mathbb{1}}$). Since $\tilde{\tau}_3$ raised to an even power is equal to $\tilde{\mathbb{1}}$, the T matrix splits into a $\tilde{\tau}_3$ component and a $\tilde{\mathbb{1}}$ component. Summing the resulting geometric series we find that

$$\tilde{T}_{jj'}=T^a_{jj'}\tilde{\tau}_3+T^b_{jj'}\tilde{\mathbb{1}},$$

$$T^a_{jj'}=\left(\frac{\underline{V}}{1-F'(i\omega)^2\underline{V}^2}\right)_{jj'},$$

$$T^b_{jj'}=\left(\frac{-F'(i\omega)\underline{V}^2}{1-F'(i\omega)^2\underline{V}^2}\right)_{jj'}, \tag{B12}$$

where

$$F'(i\omega)=\frac{F[i\omega-\Sigma(i\omega)]}{4\pi v_fv_2}, \tag{B13}$$

$$F(x)\equiv x\ln\left(1-\frac{p_0^2}{x^2}\right) \tag{B14}$$

and p_0 is the large scaled momentum cutoff defined in Sec. II.

Taking the Nambu space trace of Eq. (B6), cyclically permuting within the trace, and replacing the momentum sum with a scaled integral about the nodes via Eq. (B8) yields

$$\mathrm{Tr}\,\tilde{\Lambda}^{\alpha}=\mathrm{Tr}\Bigg[n_i\int\frac{d^2p}{(2\pi)^2 v_f v_2}\tilde{\mathcal{G}}(\mathbf{p},i\omega)\times\sum_{j=1}^{4}(\hat{\mathbf{k}}^{j'}\cdot\hat{\mathbf{k}}^{j})\tilde{T}_{jj'}(i\omega)\tilde{\tau}_{\alpha}\tilde{T}_{j'j}(i\omega+i\Omega)\times\tilde{\mathcal{G}}(\mathbf{p},i\omega+i\Omega)\tilde{\tau}_{\alpha}(\tilde{\mathbb{1}}+\tilde{\Lambda}^{\alpha})\Bigg]. \tag{B15}$$

Defining node j' to be node 1 we can write for $j=1,2,3,4$

$$\mathbf{k}^{j}=\left\{\left(\pm\frac{\pi}{2},\pm\frac{\pi}{2}\right)\right\},$$

$$\hat{\mathbf{k}}^{j'}\cdot\hat{\mathbf{k}}^{j}=\{1,0,-1,0\},$$

$$\tilde{T}_{jj'}=\tilde{T}_{j'j}\equiv\{\tilde{T}_1,\tilde{T}_2,\tilde{T}_3,\tilde{T}_2\},$$

and therefore

$$\sum_{j=1}^{4}(\hat{\mathbf{k}}^{j'}\cdot\hat{\mathbf{k}}^{j})\tilde{T}_{jj'}(i\omega)\tilde{\tau}_{\alpha}\tilde{T}_{j'j}(i\omega+i\Omega)=\tilde{T}_n(i\omega)\tilde{\tau}_{\alpha}\tilde{T}_n(i\omega+i\Omega)[|_{n=1}-|_{n=3}]=\frac{4\pi v_f v_2}{n_i}[\gamma_A^{\alpha}(i\omega,i\Omega)+\gamma_B^{\alpha}(i\omega,i\Omega)\tilde{\tau}_3]\tilde{\tau}_{\alpha}, \tag{B16}$$

where

$$\gamma_A^{\alpha}\equiv\frac{n_i}{4\pi v_f v_2}[\eta_{\alpha}T_n^a(i\omega)T_n^a(i\omega+i\Omega)+T_n^b(i\omega)T_n^b(i\omega+i\Omega)][|_{n=1}-|_{n=3}], \tag{B17}$$

$$\gamma_B^{\alpha}\equiv\frac{n_i}{4\pi v_f v_2}[\eta_{\alpha}T_n^b(i\omega)T_n^a(i\omega+i\Omega)+T_n^a(i\omega)T_n^b(i\omega+i\Omega)][|_{n=1}-|_{n=3}], \tag{B18}$$

and we define

$$\eta_{\alpha}\equiv\begin{cases}+1 & \text{for } \alpha=0,3,\\ -1 & \text{for } \alpha=1,2.\end{cases} \tag{B19}$$

Plugging Eq. (B16) into Eq. (B15) and defining

$$\tilde{I}^{\alpha}(i\omega,i\Omega)=\int\frac{d^2p}{\pi}\tilde{\mathcal{G}}(\mathbf{p},i\omega)\tilde{\tau}_{\alpha}\tilde{\mathcal{G}}(\mathbf{p},i\omega+i\Omega)\tilde{\tau}_{\alpha} \tag{B20}$$

and

$$\tilde{I}_3^{\alpha}(i\omega,i\Omega)=\int\frac{d^2p}{\pi}\tilde{\mathcal{G}}(\mathbf{p},i\omega)\tilde{\tau}_3\tilde{\tau}_{\alpha}\tilde{\mathcal{G}}(\mathbf{p},i\omega+i\Omega)\tilde{\tau}_{\alpha} \tag{B21}$$

we find that

$$\mathrm{Tr}\,\tilde{\Lambda}^{\alpha}=\mathrm{Tr}[\gamma_A^{\alpha}\tilde{I}^{\alpha}(\tilde{\mathbb{1}}+\tilde{\Lambda}^{\alpha})]+\mathrm{Tr}[\gamma_B^{\alpha}\tilde{I}_3^{\alpha}(\tilde{\mathbb{1}}+\tilde{\Lambda}^{\alpha})]. \tag{B22}$$

Similarly, multiplying Eq. (B6) by $\tilde{\tau}_3$ and repeating our steps we find that

$$\mathrm{Tr}[\tilde{\tau}_3\tilde{\Lambda}^{\alpha}]=\mathrm{Tr}[\gamma_B^{\alpha}\tilde{I}^{\alpha}(\tilde{\mathbb{1}}+\tilde{\Lambda}^{\alpha})]+\mathrm{Tr}[\gamma_A^{\alpha}\tilde{I}_3^{\alpha}(\tilde{\mathbb{1}}+\tilde{\Lambda}^{\alpha})]. \tag{B23}$$

At this point it is useful to carry out the momentum integrals in Eqs. (B20),(B21) to obtain an explicit form for $\tilde{I}^{\alpha}$ and $\tilde{I}_3^{\alpha}$. Recalling the form of the Matsubara Green's function from Sec. II, noting that $p_1=\varepsilon_k$ and $p_2=\Delta_k$, and defining

$$f_1\equiv i\omega-\Sigma(i\omega), \tag{B24a}$$

$$f_2\equiv i\omega+i\Omega-\Sigma(i\omega+i\Omega), \tag{B24b}$$

we can write

$$\tilde{\mathcal{G}}(\mathbf{p},i\omega)=\frac{f_1\tilde{\mathbb{1}}+p_1\tilde{\tau}_3+p_2\tilde{\tau}_1}{f_1^2-p^2}. \tag{B25}$$

Further, using the definition of η_{α} from Eq. (B19) and similarly defining

$$\eta'_{\alpha}\equiv\begin{cases}+1 & \text{for } \alpha=0,1,\\ -1 & \text{for } \alpha=2,3,\end{cases} \tag{B26}$$

we find that

$$\tilde{\tau}_{\alpha}\tilde{\mathcal{G}}(\mathbf{p},i\omega+i\Omega)\tilde{\tau}_{\alpha}=\frac{f_2\tilde{\mathbb{1}}+\eta_{\alpha}p_1\tilde{\tau}_3+\eta'_{\alpha}p_2\tilde{\tau}_1}{f_2^2-p^2}. \tag{B27}$$

Thus, plugging Eqs. (B25) and (B27) into Eq. (B20), noting that $p_1=p\cos\theta$ and $p_2=p\sin\theta$, and performing the angular integral we find that

$$\tilde{I}^{\alpha}=I^{\alpha}\tilde{\mathbb{1}}=\tilde{\mathbb{1}}\int_0^{p_0}2p\,\frac{f_1f_2+a_{\alpha}p^2}{(f_1^2-p^2)(f_2^2-p^2)}dp, \tag{B28}$$

where

$$a_{\alpha}\equiv\frac{\eta_{\alpha}+\eta'_{\alpha}}{2}=\begin{cases}+1 & \text{for } \alpha=0,\\ 0 & \text{for } \alpha=1,3,\\ -1 & \text{for } \alpha=2.\end{cases} \tag{B29}$$

Factoring the integrand and performing the p integral yields

$$I^{\alpha}(i\omega,i\Omega)=\frac{(f_1+a_{\alpha}f_2)F(f_2)-(f_2+a_{\alpha}f_1)F(f_1)}{f_2^2-f_1^2}, \tag{B30}$$

where $F(x)$ is defined via Eq. (B14). Similarly, acting on Eq. (B21) yields that

$$\tilde{I}_3^{\alpha}=\tilde{\tau}_3\int_0^{p_0}2p\,\frac{f_1f_2+a'_{\alpha}p^2}{(f_1^2-p^2)(f_2^2-p^2)}dp, \tag{B31}$$

where

$$a'_\alpha \equiv \frac{\eta_\alpha - \eta'_\alpha}{2} = \begin{cases} +1 & \text{for } \alpha = 3, \\ 0 & \text{for } \alpha = 0,2, \\ -1 & \text{for } \alpha = 1. \end{cases} \tag{B32}$$

It is easy to see that $a'_\alpha = a_{\alpha+1}$ (where the index addition is defined modulo 4). Hence

$$\tilde{I}^\alpha(i\omega, i\Omega) = I^\alpha \tilde{\mathbb{1}}, \tag{B33a}$$

$$\tilde{I}_3^\alpha(i\omega, i\Omega) = I^{\alpha+1} \tilde{\tau}_3, \tag{B33b}$$

where I^α is given by Eq. (B30).

Now that $\tilde{I}^\alpha$ and $\tilde{I}_3^\alpha$ have been evaluated, Eqs. (B22) and (B23) become a set of coupled equations for $\mathrm{Tr}\,\tilde{\Lambda}^\alpha$ and $\mathrm{Tr}[\tilde{\tau}_3 \tilde{\Lambda}^\alpha]$:

$$\mathrm{Tr}\,\tilde{\Lambda}^\alpha = \gamma_A^\alpha I^\alpha (2 + \mathrm{Tr}\,\tilde{\Lambda}^\alpha) + \gamma_B^\alpha I^{\alpha+1}\,\mathrm{Tr}[\tilde{\tau}_3 \tilde{\Lambda}^\alpha], \tag{B34a}$$

$$\mathrm{Tr}[\tilde{\tau}_3 \tilde{\Lambda}^\alpha] = \gamma_B^\alpha I^\alpha (2 + \mathrm{Tr}\,\tilde{\Lambda}^\alpha) + \gamma_A^\alpha I^{\alpha+1}\,\mathrm{Tr}[\tilde{\tau}_3 \tilde{\Lambda}^\alpha]. \tag{B34b}$$

Solving simultaneously yields

$$\mathrm{Tr}[\tilde{\mathbb{1}} + \tilde{\Lambda}^\alpha] = \frac{2}{1 - \gamma_A^\alpha I^\alpha \{1 + (\gamma_B^\alpha / \gamma_A^\alpha)[\gamma_B^\alpha I^{\alpha+1} / (1 - \gamma_A^\alpha I^{\alpha+1})]\}}. \tag{B35}$$

This is a very useful result since using Eqs. (B3), (B8), (B20), and (B33) with Eq. (B1) yields that

$$\overleftrightarrow{\Pi}^{gl\alpha}(i\Omega) = \frac{1}{4\pi v_f v_2} \sum_{j=1}^{4} \mathbf{v}_l^{(j)} \mathbf{v}_l^{(j)} \frac{1}{\beta} \sum_{i\omega} g^2 I^\alpha \,\mathrm{Tr}[\tilde{\mathbb{1}} + \tilde{\Lambda}^\alpha]. \tag{B36}$$

Thus plugging Eq. (B35) into Eq. (B36) and making use of Eq. (A3) from Appendix A we find that

$$\overleftrightarrow{\Pi}^{gl\alpha} = \Pi^{gl\alpha} \overleftrightarrow{\mathbb{1}}, \tag{B37}$$

where

$$\Pi^{gl\alpha}(i\Omega) = \frac{v_l^2}{\pi v_f v_2} \frac{1}{\beta} \sum_{i\omega} g^2 J^\alpha(i\omega, i\Omega), \tag{B38}$$

$$J^\alpha \equiv \frac{I^\alpha}{1 - \gamma_A^\alpha I^\alpha \{1 + (\gamma_B^\alpha / \gamma_A^\alpha)[\gamma_B^\alpha I^{\alpha+1} / (1 - \gamma_A^\alpha I^{\alpha+1})]\}} \tag{B39}$$

and we note that I^α, $I^{\alpha+1}$, γ_A^α, and γ_B^α are all functions of $i\omega$ and $i\Omega$.

Provided the input self-energy is of a proper functional form, $J^\alpha(z, i\Omega)$ will be analytic throughout the complex plane except for two branch cuts at $\mathrm{Im}\,z = 0$ and $\mathrm{Im}\,z = -\Omega$. Thus, evaluating the Matsubara sum[22] we pick up a contribution from each of the branch cuts of the summand. Consequently, it is useful to consider the form of $J^\alpha(z, i\Omega)$ above and below each of the branch cuts. Upon examination of the frequency dependence of this function via (B39),(B17)–(B21) it is clear that the internal and external frequencies, $i\omega$ and $i\Omega$, enter only through functional couplets of the form

$$P(i\omega, i\Omega) = A(i\omega) B(i\omega + i\Omega). \tag{B40}$$

Furthermore, due to the defined analytic structure of Matsubara Green's functions, the functions composing these couplets always have a Matsubara-like analytic structure and satisfy

$$A(i\omega \to \omega + i\delta) = A_{\mathrm{ret}}(\omega), \tag{B41}$$

$$A(i\omega \to \omega - i\delta) = A_{\mathrm{ret}}^*(\omega). \tag{B42}$$

Consider the form of such a couplet above and below the branch cuts of our summand. Defining

$$P_1(\omega, i\Omega) \equiv P(\omega + i\delta, i\Omega), \tag{B43a}$$

$$P_2(\omega, i\Omega) \equiv P(\omega - i\delta, i\Omega), \tag{B43b}$$

$$P_3(\omega, i\Omega) \equiv P(\omega - i\Omega + i\delta, i\Omega), \tag{B43c}$$

$$P_4(\omega, i\Omega) \equiv P(\omega - i\Omega - i\delta, i\Omega), \tag{B43d}$$

and continuing $i\Omega \to \Omega + i\delta$ we see that

$$P_3(\omega, \Omega) = P_2(\omega - \Omega, \Omega), \tag{B44a}$$

$$P_4(\omega, \Omega) = P_1^*(\omega - \Omega, \Omega). \tag{B44b}$$

Since J^α is composed of such couplets, if we similarly define

$$J_1^\alpha(\omega, i\Omega) \equiv J^\alpha(\omega + i\delta, i\Omega), \tag{B45a}$$

$$J_2^\alpha(\omega, i\Omega) \equiv J^\alpha(\omega - i\delta, i\Omega), \tag{B45b}$$

$$J_3^\alpha(\omega, i\Omega) \equiv J^\alpha(\omega - i\Omega + i\delta, i\Omega), \tag{B45c}$$

$$J_4^\alpha(\omega, i\Omega) \equiv J^\alpha(\omega - i\Omega - i\delta, i\Omega) \tag{B45d}$$

it follows that

$$J_3^\alpha(\omega, \Omega) = J_2^\alpha(\omega - \Omega, \Omega), \tag{B46a}$$

$$J_4^\alpha(\omega, \Omega) = J_1^{\alpha *}(\omega - \Omega, \Omega). \tag{B46b}$$

These relations will be very helpful in what follows. Now we can proceed with the Matsubara sum. As in Appendix A, it is best to treat the frequency-independent coupling and frequency-dependent coupling cases separately.

For $g = \{e, s\}$ (frequency-independent coupling), the sum is straightforward. Adding the contributions of the two branch cuts and using the definitions in Eq. (B45) yields

$$\Pi^{gl\alpha}(i\Omega) = i \frac{g^2}{2\pi^2} \frac{v_l^2}{v_f v_2} \int_{-\infty}^{\infty} d\omega\, n_F(\omega) \times [J_1^\alpha(\omega, i\Omega) - J_2^\alpha(\omega, i\Omega) + J_3^\alpha(\omega, i\Omega) - J_4^\alpha(\omega, i\Omega)], \tag{B47}$$

where $n_F(\omega)$ is the Fermi function.

For $g = \omega + \Omega/2$ (frequency-dependent coupling), noting the technical issues discussed in the analogous stage of the

bare bubble calculation (see Appendix A), we can proceed as above. Adding the contributions of the two branch cuts and using Eq. (B45) we find that

$$\Pi^{gl\alpha}(i\Omega)=i\frac{1}{2\pi^2}\frac{v_l^2}{v_f v_2}\int_{-\infty}^{\infty}d\omega\, n_F(\omega)\times\left[\left(\omega+\frac{i\Omega}{2}\right)^2[J_1^\alpha(\omega,i\Omega)-J_2^\alpha(\omega,i\Omega)]+\left(\omega-\frac{i\Omega}{2}\right)^2[J_3^\alpha(\omega,i\Omega)-J_4^\alpha(\omega,i\Omega)]\right]. \tag{B48}$$

In either case, continuing $i\Omega\to\Omega+i\delta$, making use of the relations in Eq. (B46), and shifting $\omega\to\omega+\Omega$ in the last two terms, we obtain the retarded polarization function

$$\Pi^{gl\alpha}_{\rm ret}(\Omega)=i\frac{1}{2\pi^2}\frac{v_l^2}{v_f v_2}\int_{-\infty}^{\infty}d\omega\, g^2\times\{n_F(\omega)[J_1^\alpha(\omega,\Omega)-J_2^\alpha(\omega,\Omega)]-n_F(\omega+\Omega)[J_1^{\alpha *}(\omega,\Omega)-J_2^\alpha(\omega,\Omega)]\} \tag{B49}$$

which is valid for all three coupling parameters. Taking the imaginary part, noting that $\mathrm{Re}[z]=\mathrm{Re}[z^*]$, and expanding J_1^α and J_2^α yields

$$\mathrm{Im}\,\Pi^{gl\alpha}_{\rm ret}(\Omega)=\frac{1}{2\pi^2}\frac{v_l^2}{v_f v_2}\int_{-\infty}^{\infty}d\omega\, g^2[n_F(\omega+\Omega)-n_F(\omega)]\times\mathrm{Re}\left[\frac{I_2^\alpha}{1-\gamma_{A2}^\alpha I_2^\alpha\{1+(\gamma_{B2}^\alpha/\gamma_{A2}^\alpha)[\gamma_{B2}^\alpha I_2^{\alpha+1}/(1-\gamma_{A2}^\alpha I_2^{\alpha+1})]\}}-\frac{I_1^\alpha}{1-\gamma_{A1}^\alpha I_1^\alpha\{1+(\gamma_{B1}^\alpha/\gamma_{A1}^\alpha)[\gamma_{B1}^\alpha I_1^{\alpha+1}/(1-\gamma_{A1}^\alpha I_1^{\alpha+1})]\}}\right], \tag{B50}$$

where

$$I_1^\alpha(\omega,\Omega)=\frac{(f_1+a_\alpha f_2)F(f_2)-(f_2+a_\alpha f_1)F(f_1)}{f_2^2-f_1^2}, \tag{B51}$$

$$I_2^\alpha(\omega,\Omega)=\frac{(f_1^*+a_\alpha f_2)F(f_2)-(f_2+a_\alpha f_1^*)F(f_1^*)}{f_2^2-f_1^{*2}}, \tag{B52}$$

$$f_1=\omega-\Sigma_{\rm ret}(\omega), \tag{B53a}$$

$$f_2=\omega+\Omega-\Sigma_{\rm ret}(\omega+\Omega). \tag{B53b}$$

$$\gamma_{A1}^\alpha\equiv\frac{n_i}{4\pi v_f v_2}[\eta_\alpha T_n^a(\omega)T_n^a(\omega+\Omega)+T_n^b(\omega)T_n^b(\omega+\Omega)][|_{n=1}-|_{n=3}], \tag{B54}$$

$$\gamma_{A2}^\alpha\equiv\frac{n_i}{4\pi v_f v_2}[\eta_\alpha T_n^a(\omega)^*\,T_n^a(\omega+\Omega)+T_n^b(\omega)^*\,T_n^b(\omega+\Omega)][|_{n=1}-|_{n=3}], \tag{B55}$$

$$\gamma_{B1}^\alpha\equiv\frac{n_i}{4\pi v_f v_2}[\eta_\alpha T_n^b(\omega)T_n^a(\omega+\Omega)+T_n^a(\omega)T_n^b(\omega+\Omega)][|_{n=1}-|_{n=3}], \tag{B56}$$

$$\gamma_{B2}^\alpha\equiv\frac{n_i}{4\pi v_f v_2}[\eta_\alpha T_n^b(\omega)^*\,T_n^a(\omega+\Omega)+T_n^a(\omega)^*\,T_n^b(\omega+\Omega)][|_{n=1}-|_{n=3}], \tag{B57}$$

$$T_n^a(\omega)=\left(\frac{\underline{V}}{1-F'(\omega)^2\underline{V}^2}\right)_{n1}, \tag{B58}$$

$$T_n^b(\omega)=\left(\frac{-F'(\omega)\underline{V}^2}{1-F'(\omega)^2\underline{V}^2}\right)_{n1}, \tag{B59}$$

$$F'(\omega)=\frac{F[\omega-\Sigma_{\rm ret}(\omega)]}{4\pi v_f v_2}, \tag{B60}$$

and $F(x)$ is defined in Eq. (B14). The above equations define the imaginary part of the generalized retarded polarization function including ladder corrections to the vertex. By specifying different input parameters we can use it to obtain the electrical, thermal, and spin conductivity.

APPENDIX C: NUMERICAL ANALYSIS OF UNIVERSAL LIMIT VERTEX CORRECTIONS

In Secs. III C, IV C, and V C, the vertex correction factors for the universal limit electrical and thermal/spin conductivities were found to be

$$\beta_{\rm VC}=\frac{1+2[\gamma_{A2}^{(0)}-\gamma_{A1}^{(0)}+\gamma_{B1}^{(0)^2}/(1-\gamma_{A1}^{(0)})]\ln(p_0/\Gamma_0)[\ln(p_0/\Gamma_0)-1]}{[1-2\gamma_{A2}^{(0)}\ln(p_0/\Gamma_0)]\{1-2[\gamma_{A1}^{(0)}-\gamma_{B1}^{(0)^2}/(1-\gamma_{A1}^{(0)})][\ln(p_0/\Gamma_0)-1]\}},\tag{C1}$$

$$\beta_{\rm VC}^{T,s}=\frac{1/2}{1-\gamma_{A2}^{(0)}}+\frac{1/2}{1+\gamma_{A1}^{(0)}(1+(\gamma_{B1}^{(0)}/\gamma_{A1}^{(0)})\{\gamma_{B1}^{(0)}[2\ln(p_0/\Gamma_0)-2]/[1-\gamma_{A1}^{(0)}/2\ln(p_0/\Gamma_0)-2]]\})},\tag{C2}$$

where the γ's and their constituent functions are given in Eqs. (3.14)–(3.17). Here we shall numerically compute both factors as a function of impurity density and scattering potential. To facilitate the computation, it is convenient to make all quantities dimensionless by expressing energies in units of p_0 and lengths in units of $2a$. This choice of units sets the frequently encountered constant, $4\pi v_f v_2$, equal to 1. For a particular set of input parameters, the computation is done in two steps. First, solve self-consistently for the zero-frequency scattering rate Γ_0 via

$$\Sigma_{\rm ret}(\omega)=n_i T_{11}^b(\omega),\tag{C3}$$

which (in the universal limit with our choice of units) reduces to

$$2n_i\ln\frac{1}{\Gamma_0}\left(\frac{\underline{V}^2}{1+[2\Gamma_0\ln(1/\Gamma_0)]^2\underline{V}^2}\right)_{1,1}=1.\tag{C4}$$

Then given Γ_0, plug into Eqs. (C1) and (C2) to obtain the vertex corrections.

The result will depend on the set of four input parameters which determine the impurity density and scattering potential $\{n_i,V_1,V_2,V_3\}$. In our units, $n_i=4z$ where z is the substitutional fraction of impurities. Furthermore, it is convenient to parametrize the scattering potential via

$$V_1=V_{\rm scale}\tan\left(\frac{\pi}{2}d\right),\quad R_2=\frac{V_2}{V_1},\quad R_3=\frac{V_3}{V_1},\tag{C5}$$

where $V_{\rm scale}$ is a dimensionless constant and d ranges from 0 to 1. Hence, the scattering anisotropy is given by R_2 and R_3 while the scattering strength is given by d. Note that while it is tempting to think of $(\pi/2)d$ as some sort of scattering phase shift, to do so would be stretching an analogy beyond its realm of usefulness. The above is merely a helpful parametrization, the aim of which is to allow us to go smoothly from the Born limit to the unitary limit as d varies from 0 to 1. For our purposes, these limits are determined by the denominator in Eq. (C4):

$$\left(2\Gamma_0\ln\frac{1}{\Gamma_0}\right)V_1\ll 1\rightarrow\text{Born limit},$$

$$\left(2\Gamma_0\ln\frac{1}{\Gamma_0}\right)V_1\gg 1\rightarrow\text{unitary limit}.$$

Thus, for a particular range of z, we shall set $V_{\rm scale}$ to a value that allows us to evenly sample the transition from one limit to the other. In the end, these manipulations yield a new set of four dimensionless input parameters $\{z,d,R_2,R_3\}$.

The electrical and thermal/spin vertex corrections obtained for a typical set of input parameters, via the procedure described above, are plotted in Fig. 5. Here we have assumed that $V(\mathbf{k})$ falls off slowly with increasing $\mathbf{k}$ ($R_2=0.9$, $R_3=0.8$) and have plotted the vertex corrections versus impurity fraction ($z=0.01\%\rightarrow 1\%$) for seven scattering strengths from Born ($d=0.001$) to unitary ($d=0.999$). Note that the electrical correction, $\beta_{\rm VC}-1$, can be quite significant while the thermal/spin correction, $\beta_{\rm VC}^{T,s}-1$, is much smaller and vanishes as $z\rightarrow 0$. The difference between the two cases is seen most clearly in Fig. 6 where, for $d=0.001,0.5,0.999$, we have replotted the electrical and thermal/spin correction factors on the same scale. On the scale of $\beta_{\rm VC}-1$, it is difficult to distinguish $\beta_{\rm VC}^{T,s}-1$ from the x axis. Thus, we see that for all scattering strengths, the thermal/spin vertex correction is negligible compared to the electrical vertex correction.

Additional insight is gained through consideration of the intermediate stages of the calculation which reveal that

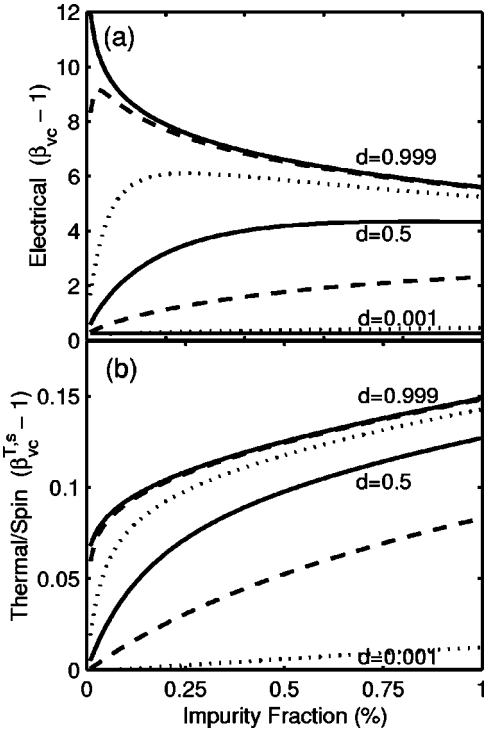

FIG. 5. Numerically calculated (a) electrical and (b) thermal/spin vertex corrections plotted as a function of impurity fraction ($z=0.01\%\rightarrow 1\%$) for scattering strengths parametrized via (from bottom to top) $d=\{0.001$(Born), 0.1, 0.3, 0.5, 0.7, 0.9, 0.999 (unitary)$\}$. In all cases we have set $V_{\rm scale}=20$ and assumed that $V(\mathbf{k})$ falls off slowly with $|\mathbf{k}|$ ($R_2=0.9$, $R_3=0.8$).

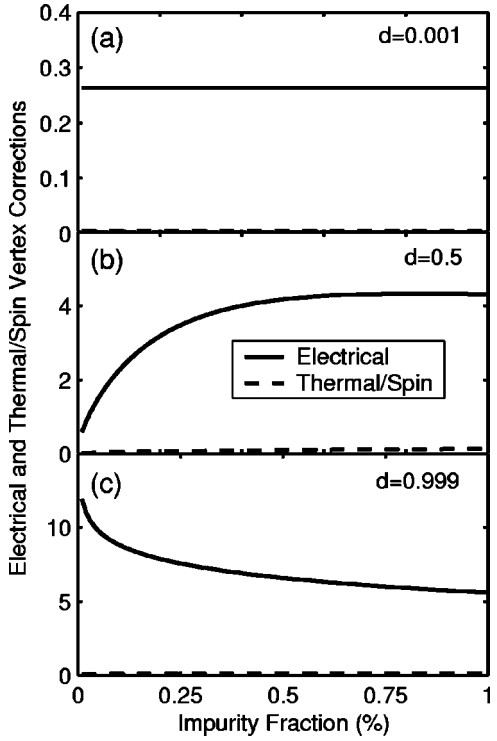

FIG. 6. Direct comparison of electrical ($\beta_{\mathrm{VC}}-1$) and thermal/spin ($\beta_{\mathrm{VC}}^{T,s}-1$) vertex corrections for (a) $d=0.001$, (b) $d=0.5$, and (c) $d=0.999$. Note that in all cases, the thermal/spin correction is negligible on the scale of of the electrical correction.

$$\gamma_{A1}^{(0)},\gamma_{A2}^{(0)},\gamma_{B1}^{(0)}\lesssim\mathcal{O}\left(\frac{1}{\ln(p_0/\Gamma_0)}\right). \tag{C6}$$

In the Born limit, $1/\ln(p_0/\Gamma_0)\sim z$, which can truly be neglected for the small impurity fractions of interest. In the unitary limit, $1/\ln(p_0/\Gamma_0)\sim 1/\ln(1/z)$, which vanishes much more slowly but is still small compared to terms of order unity. Thus, since we can treat the γ's as small quantities, the (mathematical) difference between the electrical and thermal/spin cases is due to the manner in which the γ's enter Eqs. (C1) and (C2). The γ's enter β_{VC} within order unity combinations of the form $\gamma\ln(p_0/\Gamma_0)$ [and for some parameter values even $\gamma\ln^2(p_0/\Gamma_0)$] which cannot be neglected. In contrast, the γ's enter $\beta_{\mathrm{VC}}^{T,s}$ on their own (that is, in direct competition with terms of order unity) and can therefore be neglected for small z. Hence we say that electrical vertex corrections contribute even to zeroth order in the impurity density while thermal/spin vertex corrections do not.

APPENDIX D: FERMI-LIQUID CORRECTIONS

In addition to the effects of vertex corrections, transport coefficients may be further modified due to underlying Fermi-liquid interactions between Landau quasiparticles (referred to hereafter as ''electrons'' to avoid any confusion with the Bogoliubov quasiparticle excitations of the superconductor). A detailed theory of the superfluid Fermi liquid has been developed in the literature.[9,10,28–30] In particular, a widely applicable phenomenological approach has been devised by Leggett.[28] Within this approach, we consider three layers of Fermi-liquid effects. (1) Mass renormalization: By virtue of our acknowledgment that ''electrons'' are really Landau quasiparticles, all masses should be viewed as effective masses m^*. (2) Current renormalization: Due to Fermi-liquid interactions, the presence of a current yields an additional drag current resulting in an overall current renormalization. (3) Response function modification: Fermi-liquid interactions induce an effective ''molecular field'' which couples to the current-producing perturbation and modifies the response function $K_0(T)$ via

$$K_0(T)\rightarrow K(T)=\frac{K_0(T)}{1+\lambda K_0(T)}, \tag{D1}$$

where λ is a constant which depends on the interaction.[28] In the case at hand, (1) has been built into the parameters of our model, (2) yields a nontrivial effect which shall be considered below, and (3) can be neglected in the $T\rightarrow 0$ limit with which we are concerned. This last statement follows because at low T, few quasiparticles are generated, response functions (such as the normal fluid density or conductivity) are small, and the higher order correction terms in Eq. (D1) are negligible. Thus, the dominant corrections to transport coefficients due to Fermi-liquid interactions enter simply via renormalization of the various current density operators. To determine the nature of this current renormalization, we proceed as follows.[31]

In the absence of Fermi-liquid interactions, a generic (bare) current density operator takes the form

$$\mathbf{j}_0=\sum_{k\alpha} g_{k\alpha}\mathbf{v}_k\,\delta n_{k\alpha}, \tag{D2}$$

where $\mathbf{v}_k$ is a velocity, $g_{k\alpha}$ is a coupling parameter (i.e., charge, spin, or energy), and

$$\delta n_{k\alpha}=n_{k\alpha}-n_0(\epsilon_k,\Delta_k) \tag{D3}$$

is the difference between the true electron distribution in the presence of the current-inducing perturbation $n_{k\alpha}$ and the (bare) equilibrium distribution $n_0(\epsilon_k,\Delta_k)$. (The *bare* designations refer to our neglect of Fermi-liquid interactions aside from the extent to which they are included in the velocity via mass renormalization.)

Once Fermi-liquid interactions are turned on, excited electrons interact via the Landau interaction energy $f_{kk'}^{\alpha\alpha'}$. In the presence of this interaction, the electron dispersion must be modified (or dressed) to account for the additional energy cost of interacting with other excited electrons:

$$\tilde{\epsilon}_k=\epsilon_k+\sum_{k'\alpha'} f_{kk'}^{\alpha\alpha'}\,\delta n_{k'\alpha'}. \tag{D4}$$

(Note that in this context, the tilde denotes a dressed quantity, not a Nambu matrix.) It is important to realize that the dispersion of *every* electron (not just the excited ones) is dressed as long as any electrons are excited. Although only the excited electrons interact, the dispersion measures the energy required to excite an electron and must therefore account for the interactions an electron *would* experience if it were excited. Also note that although Δ_k should also be modified due to Fermi-liquid interactions, we expect this effect to be less significant and shall therefore assume for the sake of simplicity that the gap is unaffected. Once the dis-

persion is dressed, we can Taylor expand in the change in ϵ_k to obtain a dressed equilibrium distribution function

$$n_0(\tilde{\epsilon}_k,\Delta_k)=n_0(\epsilon_k,\Delta_k)+\frac{\partial n_0}{\partial \epsilon_k}\sum_{k'\alpha'} f_{kk'}^{\alpha\alpha'}\,\delta n_{k'\alpha'}. \quad \text{(D5)}$$

Thus, the dressed current density operator takes the form

$$\mathbf{j}=\sum_{k\alpha} g_{k\alpha}\mathbf{v}_k\,\delta\tilde{n}_{k\alpha}, \quad \text{(D6)}$$

where

$$\delta\tilde{n}_{k\alpha}=\delta n_{k\alpha}-\frac{\partial n_0}{\partial \epsilon_k}\sum_{k'\alpha'} f_{kk'}^{\alpha\alpha'}\,\delta n_{k'\alpha'} \quad \text{(D7)}$$

is the difference between the true electron distribution and the equilibrium distribution in the presence of Fermi-liquid interactions.

In a superconductor, there are two types of electrons: those that compose the condensate of ground state pairs and those that form the Bogoliubov quasiparticles. Hence the equilibrium distribution function has both a condensate term and a quasiparticle term

$$n_0=n_0^C+n_0^Q. \quad \text{(D8)}$$

The equilibrium distribution of electrons in the condensate is just given by the coherence factor v_k^2 so its derivative is

$$\frac{\partial n_0^C}{\partial \epsilon_k}=\frac{\partial}{\partial \epsilon_k}\left[\frac{1}{2}\left(1-\frac{\epsilon_k}{E_k}\right)\right]=-\frac{\Delta_k^2}{2E_k^3}. \quad \text{(D9)}$$

In the presence of impurities, the equilibrium quasiparticle distribution is given by the convolution of the quasiparticle spectral function (a Lorentzian of width Γ_0 about E_k) and the Fermi function n_F. Multiplying this by the probability the quasiparticle is an electron minus the probability it is a hole ($u_k^2-v_k^2$), we obtain the equilibrium distribution of electrons that form the quasiparticles. In the $T\ll\Gamma_0$ limit, its derivative is given by

$$\frac{\partial n_0^Q}{\partial \epsilon_k}=\frac{\partial}{\partial \epsilon_k}\left[\frac{\epsilon_k}{E_k}\int_{-\infty}^{\infty} d\omega\,\frac{\Gamma_0/\pi}{(\omega-E_k)^2+\Gamma_0^2}n_F(\omega)\right]$$
$$=-\frac{\epsilon_k^2}{E_k^2}\frac{\Gamma_0/\pi}{E_k^2+\Gamma_0^2}+\frac{\Delta_k^2}{\pi E_k^3}\arctan\left(\frac{\Gamma_0}{E_k}\right). \quad \text{(D10)}$$

Making use of these expressions and evaluating the dressed current density operator

$$\mathbf{j}=\sum_{k\alpha} g_{k\alpha}\mathbf{v}_k\left[\delta n_{k\alpha}-\left(\frac{\partial n_0^C}{\partial \epsilon_k}+\frac{\partial n_0^Q}{\partial \epsilon_k}\right)\sum_{k'\alpha'} f_{kk'}^{\alpha\alpha'}\,\delta n_{k'\alpha'}\right] \quad \text{(D11)}$$

for the appropriate coupling parameters and velocities, the Fermi-liquid renormalizations of the electrical, thermal, and spin currents can be computed.

[1] P. A. Lee, Phys. Rev. Lett. **71**, 1887 (1993).
[2] P. J. Hirschfeld, W. O. Putikka, and D. J. Scalapino, Phys. Rev. Lett. **71**, 3705 (1993).
[3] P. J. Hirschfeld, W. O. Putikka, and D. J. Scalapino, Phys. Rev. B **50**, 10 250 (1994).
[4] P. J. Hirschfeld and W. O. Putikka, Phys. Rev. Lett. **77**, 3909 (1996).
[5] M. J. Graf, S-K. Yip, J. A. Sauls, and D. Rainer, Phys. Rev. B **53**, 15 147 (1996).
[6] T. Senthil, M. P. A. Fisher, L. Balents, and C. Nayak, cond-mat/9808001 (unpublished).
[7] A. V. Balatsky, A. Rosengren, and B. L. Altshuler, Phys. Rev. Lett. **73**, 720 (1994).
[8] P. A. Lee and X. G. Wen, Phys. Rev. Lett. **78**, 4111 (1997).
[9] A. J. Millis, S. M. Girvin, L. B. Ioffe, and A. I. Larkin, J. Phys. Chem. Solids **59**, 1742 (1998).
[10] D. Xu, S. K. Yip, and J. A. Sauls, Phys. Rev. B **51**, 16 233 (1995).
[11] A. Hosseini, R. Harris, S. Kamal, P. Preston, R. Liang, W. N. Hardy, and D. A. Bonn, cond-mat/9811041 (unpublished).
[12] L. Taillefer, B. Lussier, R. Gagnon, K. Behnia, and H. Aubin, Phys. Rev. Lett. **79**, 483 (1997).
[13] M. Chiao, R. W. Hill, C. Lupien, B. Popic, R. Gagnon, and L. Taillefer, Phys. Rev. Lett. **82**, 2943 (1999).
[14] D. A. Bonn, S. Kamal, A. Bonakdarpour, R. Liang, W. N. Hardy, C. C. Holmes, D. N. Basov, and T. Timusk, Czech. J. Phys. **46**, 3195 (1996).
[15] J. Mesot, M. R. Norman, H. Ding, M. Randeria, J. C. Campuzano, A. Paramekanti, H. M. Fretwell, A. Kaminski, T. Takeuchi, T. Yokoya, T. Sato, T. Takahashi, T. Mochiku, and K. Kadowaki, cond-mat/9812377 (unpublished).
[16] L. P. Gorkov and P. A. Kalugin, Pis'ma Zh. Éksp. Teor. Fiz. **41**, 208 (1985) [JETP Lett. **41**, 253 (1985)].
[17] A. A. Nersesyan, A. M. Tsvelik, and F. Wenger, Nucl. Phys. B **438**, 561 (1995).
[18] T. Senthil and M. P. A. Fisher, cond-mat/9810238 (unpublished).
[19] V. Ambegaokar and A. Griffin, Phys. Rev. A **137**, A1151 (1965).
[20] V. Ambegaokar and L. Tewordt, Phys. Rev. A **134**, A805 (1964).
[21] J. R. Schrieffer, *Theory of Superconductivity* (Addison-Wesley, Reading, MA, 1964).
[22] G. D. Mahan, *Many-Particle Physics* (Plenum, New York, 1990).
[23] H. Monien, K. Scharnberg, and D. Walker, Solid State Commun. **63**, 263 (1987).
[24] P. J. Hirschfeld, P. Wölfle, and D. Einzel, Phys. Rev. B **37**, 83 (1988).
[25] J. Moreno and P. Coleman, cond-mat/9603079 (unpublished).
[26] M. Chiao, P. Lambert, R. W. Hill, C. Lupien, R. Gagnon, L. Taillefer, and P. Fournier, cond-mat/9910367 (unpublished).
[27] S. F. Lee, D. C. Morgan, R. J. Ormeno, D. M. Broun, R. A. Doyle, and J. R. Waldram, Phys. Rev. Lett. **77**, 735 (1996).
[28] A. J. Leggett, Phys. Rev. **140**, A1869 (1965).
[29] A. I. Larkin and A. B. Migdal, Zh. Éksp. Teor. Fiz. **44**, 1703 (1963) [JETP Lett. **17**, 1146 (1963)].
[30] A. I. Larkin, Zh. Éksp. Teor. Fiz. **46**, 2188 (1964) [JETP Lett. **19**, 1478 (1964)].
[31] D. Pines and P. Nozieres, *The Theory of Quantum Liquids* (Addison-Wesley, Reading, MA, 1966).